A WIDEBAND DOUBLE RIDGE GUIDE HORN ANTENNA AS COMPLEX ANTENNA TRANSFER FUNCTION STANDARD

by

Mariesa Nel

Submitted in partial fulfilment of the requirements for the degree
Master of Engineering (Electronic Engineering)

in the

Department of Electrical, Electronic and Computer Engineering
Faculty of Engineering, the Built Environment and Information Technology

UNIVERSITY OF PRETORIA

April 2013

SUMMARY

A WIDEBAND DOUBLE RIDGE GUIDE HORN ANTENNA AS COMPLEX ANTENNA TRANSFER FUNCTION STANDARD

by

Mariesa Nel

Supervisor: Prof. J. Joubert

Co-supervisor: Prof. J. W. Odendaal

Department: Electrical, Electronic and Computer Engineering

University: University of Pretoria

Degree: Master of Engineering (Electronic Engineering)

Keywords: Double ridge guide horn antenna, complex antenna transfer function, time domain, frequency domain, compact antenna test range, anechoic chamber, standard antenna, uncertainties.

Ultra wideband (UWB) technology plays a significant role in wireless communication. The complex antenna transfer function (CATF) of an UWB antenna provides important information required for better channel designs and communication systems. In this dissertation the CATF of a Double ridge guide horn (DRGH) antenna is determined and used as a standard antenna for UWB measurements. Two methods were used: the two antenna method in an anechoic chamber and a modified gain-transfer method in a compact antenna test range (CATR). Measurements were performed with a vector network analyser (VNA) in the frequency domain, in the anechoic chamber and the CATR. The distance measurements required to calculate the CATF from the S-parameter measurements were performed in the time domain. The CATF of the standard antenna was determined using two identical antennas and then it was shown that a modified gain-transfer method can be used to determine the CATF of any unknown antenna in a CATR, using the standard antenna as a reference. Some of the challenges were to obtain the correct equations and measurement method to obtain the CATF in a CATR. The standard antenna was used to investigate uncertainty contributions for the measurements in the CATR.

OPSOMMING

'N WYEBAND DUBBEL-RIF GOLFLEIER-HORING ANTENNE AS 'N KOMPLEKSE ANTENNE-OORDRAGSFUNKSIE STANDAARD

deur

Mariesa Nel

Studieleier: Prof. J. Joubert

Mede-studieleier: Prof. J. W. Odendaal

Departement: Elektriese, Elektroniese en Rekenaar Ingenieurswese

Universiteit: Universiteit van Pretoria

Graad: Magister in Ingenieurswese (Elektroniese Ingenieurswese)

Sleutelwoorde: Dubbel-rif golfleier-horing antenne, komplekse antenne-oordragsfunksie, tyddomein, frekwensiedomein, kompakte antenne-meetbaan, anechoiese kamer, standaard antenna, onsekerhede.

Ultrawyeband tegnologie speel 'n belangrike rol in moderne kommunikasiestelsels. Die komplekse antenne-oordragsfunksie (KAO) van 'n ultrawyeband antenne bevat belangrike inligting wat gebruik kan word om kommunikasiestelsels beter te ontwerp. In hierdie verhandeling word die KAO van 'n dubbel-rif golfleier-horing (DRGH) antenne bepaal en dan gebruik word as 'n standard antenne vir ultrawyeband meetings. Twee metodes was gebruik om die KAO te bepaal: die twee-antenne metode in 'n anechoïese kamer, asook 'n aangepasde winsoordragsmetode in 'n kompakte antenne-meetbaan. Frekwensiedomein S-parameter metings is met 'n vektor-netwerkanaliseerder geneem. Die afstand tussen die twee antennes was in die tyddomein gemeet. Die KOA van die standaard antenna is bepaal deur twee identiese antennas te gebruik, en daarna word gewys dat 'n aangepasde winsoordragsmetode gebruik kan word om die KOA van enige onbekende antenne in 'n kompakte antenne-meetbaan te bepaal. Van die uitdagings was die daarstel van 'n geskikte meetmetode en die korrekte vergelyking om die KAO in die kompakte antenne-meetbaan bepaal. 'n Onsekerheids-analise is gedoen vir die metings in die kompakte antenne-meetbaan, deur gebruik te maak van die standaard antenne.

ACKNOWLEDGEMENTS

I would like to acknowledge the National Metrology Institute of South Africa (NMISA) for the support during my studies.

Bennie Jacobs, at SAAB, for providing some of the antennas.

I would like to thank the Lord Jesus my Christ and Saviour for giving me the mind, ability and opportunity to complete my Masters degree.

To my husband, Riaan Nel, for support and love throughout the years.

LIST OF ABBREVIATIONS

AF	Antenna factor
CAF	Complex antenna factor
CATF	Complex antenna transfer function
CATR	Compact antenna test range
DRGH	Double ridge guide horn
ESDM	Estimated standard deviation of the mean
NM	Type-N Male
SMA (F)	Sub-Miniature version A Female
SMA (M)	Sub-Miniature version A Male
UWB	Ultra wideband
VNA	Vector network analyser
VRC	Voltage reflection coefficient
VSWR	Voltage standing wave ratio

TABLE OF CONTENTS

CHAPTER 1 INTRODUCTION

1.1. BACKGROUND AND MOTIVATION

Antennas are an essential part of wireless communication. Ultra wideband (UWB) technology has received worldwide attention since the allocation of a specific frequency band that can be used for ultra wideband communication [1]. The purpose of this research was to obtain the complex antenna transfer function (CATF) of an UWB antenna, and then to show that such an antenna can be used as an UWB measurement standard to characterise other antennas in terms of their CATF in a compact antenna test range (CATR) facility. The approach used in this dissertation is based on frequency domain measurements.

Ultra wideband communication for wireless technology promises high data rates and low power consumption. Wireless technology is also moving into the indoor environment, [2], where antenna systems also need to be evaluated and designed for efficiency. A test facility will be required where these antennas can be characterised. An UWB antenna system can efficiently be designed for optimum performance with the aid of the CATF of an antenna and not only the general electrical properties (gain, radiation pattern, efficiency, effective area and polarisation) [1]. For wider bandwidths, these properties of an antenna become highly dependent on frequency and cannot be evaluated as easily as in the case of narrow band applications [1].

The transfer function can be obtained by experimental measurements [3, 4], or numerical simulations [5, 6], and by either analysing the measurements in the frequency domain or time domain. Authors used these different methods and techniques to obtain the transfer functions of a variety of antennas e.g., monopoles, dipoles, Vivaldi antenna and Quad ridge horn antennas.

The authors in [4] use the equivalent circuit to obtain the transfer function of an UWB antenna, and used the ABCD-parameters and measured in the time domain to describe the equivalent circuit. Subsequent research by [7] shows that S-parameters, which can be easily measured with a VNA, is preferred above using ABCD-parameter.

Channel transfer modelling is described by [5, 8 – 12] where the transmit antenna transfer function, channel transfer function and a receive antenna transfer function, on a number of different antennas were determined. In [5] the frequency domain measurements were compared to the numerical calculations. The authors in [8] used a slightly modified method to obtain the transmit-, receive- and channel transfer function. By using this method the transfer function of transmit- and receive- antenna is free from the influences of the channel. Directional transfer functions, as well as the channel transfer function, were also determined by the authors in [9 – 11]. The measurements were performed in the frequency domain and the antennas were placed at different angles from one another. The authors of [13] obtained the impulse response through the corresponding time domain wave form (of an antenna) which reflects the contribution of both transmit- and receive-antenna and channel in the link.

The complex antenna factor (CAF) of an UWB antenna is also a common way to characterise these antennas [14 – 19]. The CAF includes the phase values in addition to the conventional scalar antenna factor (AF). The three antenna method in the near field was used to calculate the CAF in the far-field region of an antenna, as evaluated in literature [6, 17, 18]. The authors in [15] used simulations and measurements to calculate the CAF. This paper also provides more detail on error estimation of the CAF measurements.

The authors in [1, 3, 20, 21] used two identical antennas and performed frequency domain measurements to obtain the S-parameters and calculate the complex antenna transfer function (CATF) of one of the antennas. In [22] the three antenna method was used to measure an unknown antenna to retrieve its transfer function. When calculating the transfer function using this approach, the distance between the antennas is a vital input into the equation. The importance of the distance between the antennas was discussed when the CATF of the antenna is calculated. The authors in [20, 21] used two identical antennas and an unknown antenna with a modified three antenna method measuring in the frequency domain.

Limitations of all of the above methods and techniques, as summarised above are performed in an anechoic chamber. Measurements are performed in the near field and then

converted to far-field, or measured in the far-field directly. The three antenna method is a common method used to determine the transfer function of an unknown antenna, but is very dependent on the distance between the antennas which needs to be measured accurately.

The compact antenna test range (CATR) at the Centre of Electromagnetism, University of Pretoria, is an ideal place to set up a facility that can characterise UWB antennas, seeing that the CATR is already an established facility in the measurement of general properties of antennas in the frequency range 2 - 18 GHz.

One of the major challenges is to implement a measurement method in a CATR to determine the CATF of an unknown antenna using a standard antenna. The reflector and a feed antenna in a CATR represent the transmit antenna. A challenge is to determine how the reflector needs to be taken into account and what effect it has on the equations, as it will always be a part of the transmit antenna.

The research is limited to finding the CATF of a double ridged guide horn (DRGH) antenna, based on measurements in the frequency domain. Different UWB DRGH antennas were used to verify that the equations, measurements and methods are correct.

1.2. SCOPE AND OBJECTIVES

As mentioned in the previous section, the CATF of UWB antennas were previously primarily determined by using two identical antennas in an anechoic chamber. In this dissertation a modified gain-transfer measurement technique, using an UWB standard antenna, is shown to be a promising alternative for finding the CATF of UWB antennas. To this end the following detailed objectives were defined:

Determination of the CATF of an UWB DRGH antenna: The CATF of an UWB antenna, in this case a 2-18 GHz DRGH antenna, was to be obtained. The CATF of an antenna gives the magnitude and the phase information of the antenna – the CATF is therefore a complex quantity. The transfer function of the antenna can be obtained through measurement of two identical antennas in an anechoic chamber, or by simulation using

full-wave electromagnetic analysis software. The DRGH is suitable for UWB applications, and is appropriate to use as a standard antenna in a compact antenna test range.

Use of the standard antenna for measurements in a CATR: Once the CATF of the DRGH antenna is known, by measurement or simulation as in the previous objective, this antenna can now be used as a standard antenna. Antennas for which the CATF is unknown can be measured against the standard antenna in a CATR, as an alternative measurement technique for characterising UWB antennas in terms of their CATF. The goal of this study was not to necessarily determine the CATF of different types of antennas, but rather to focus on a specific UWB antenna, the DRGH antenna, as a standard antenna to be used in a CATR measurement facility.

1.3. ORIGINAL CONTRIBUTIONS

The complex antenna transfer function of a UWB DRGH antenna was determined: As part of the study a CATF for a DRGH antenna was determined. The DRGH antenna was designed by B. Jacobs [23] in FEKO [24]. The numerical results were obtained from FEKO simulations. The equation used to determine the transfer function of the UWB antenna was obtained from [1]. When comparing the simulated data, using the numerical models, to measured data (using two identical antennas in an anechoic chamber), excellent agreement was observed.

A modified gain-transfer measurement technique to characterise UWB antennas in terms of their CATF in a CATR was implemented: Measurements to determine the CATF of an unknown antenna are performed in the CATR, using a UWB standard antenna as the reference. An equation was derived to calculate the CATF from the complex measured S-parameters. The results were compared to simulations and measurements using the two antenna measurement method, and the comparison between the sets of data was found to be good. A study of uncertainty contributions was also done.

1.4. OVERVIEW OF THE DISSERTATION

The organisation of the dissertation is as follows:

Chapter 2: A literature study presents background on previously published progress on different approaches and techniques used to characterise antennas and to establish a transfer function for an antenna.

Chapter 3: DRGH antennas were measured using two identical antennas and the two antenna measurement method in an anechoic chamber. The CATF of these antennas were determined using equations obtained from literature. Numerical models of antennas were simulated in FEKO, and results were compared to the measured results. The results compared well and served as validation for the equations and the measurements which were performed.

Chapter 4: A DRGH antenna was used as standard antenna and the CATF of unknown antennas were determined from measurements in the CATR. A modified gain-transfer method was implemented to perform the necessary measurements. Details on the derivation of the equation to determine the CATF of an unknown antenna are given.

Chapter 5: The dissertation is concluded in this chapter. A summary of the contributions made in the dissertation and possible future work are also included in this chapter.

CHAPTER 2 BACKGROUND

2.1. INTRODUCTION

The main focus of the dissertation is to determine the complex antenna transfer function (CATF) of an ultra-wideband (UWB) antenna using frequency domain measurements – which can then be used as UWB measurement standard in a compact antenna test range (CATR). This chapter presents background information on various aspects relevant to the topic. Section 2.2 discusses different measurement methods available to measure antenna gain in general, but also the required parameters to specifically obtain the CATF of an antenna. In Section 2.3 some background and the difference between complex antenna factor (CAF) and complex antenna transfer function (CATF) are discussed. A summary of previous research related to the determination of CAF and/or CATF using frequency or time domain measurements is given in Section 2.4. The chapter is concluded in Section 2.5.

2.2. RADIATED FIELD MEASUREMENT METHODS FOR ANTENNAS

There are mainly three radiated field measurement methods for antennas which are referred to throughout the dissertation. The two antenna method is normally used in an anechoic chamber, where two identical antennas are used to determine the gain, CAF or CATF of an antenna. The three antenna method is used when two identical antennas are not available and three different antennas are needed to determine the characteristics of one or all of the antennas. The gain-transfer method is also discussed, because gain measurements in a CATR are performed using this method. A modification to the gain-transfer method is introduced later in the dissertation when the CATF (as opposed to the gain) of the DRGH antenna is determined.

2.2.1. Two antenna method

The two antenna method requires two antennas – they must either be identical, or if they are different from each other, the gain of one of the antennas should be known [25]. A typical measurement setup is shown in Figure 2.1. By using the Friis transmission formula the gain (if the two antennas are not identical) can be determined by [26]:

$$(G_A)_{dB} + (G_B)_{dB} = 20\log\left(\frac{4\pi r}{\lambda}\right) - 10\log\left(\frac{P_0}{P_r}\right), \quad (2.1)$$

where $(G_A)_{dB}$ and $(G_B)_{dB}$ are the gain in dB of antenna A and B respectively, R is the distance between the two antennas, λ the wavelength, P_0 is the transmit power and P_r the receive power and thus $\frac{P_0}{P_r}$ the measured power ratio between the two antennas.

If the two antennas are exactly the same the following equation can be used to determine the gain of the antennas:

$$(G_A)_{dB} = (G_B)_{dB} = \frac{1}{2}\left[20\log\left(\frac{4\pi r}{\lambda}\right) - 10\log\left(\frac{P_0}{P_r}\right)\right] \quad (2.2)$$

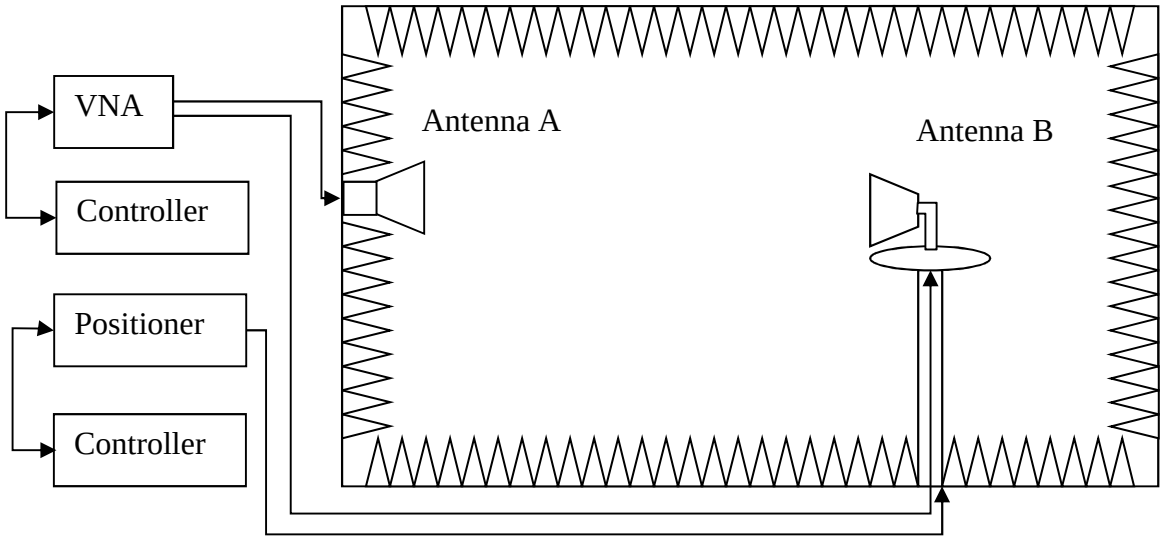

Figure 2.1. Transmission measurement setup in an anechoic chamber [1].

2.2.2. Three antenna method

The three antenna gains measurement method is used when a standard gain antenna or two identical antennas are not available [26]. Three measurements are required, and two antennas are measured at a time, as depicted in Figure 2.2. By doing three measurements, the three unknown parameters can be determined from the resulting three equations:

$$(G_1)_{dB} + (G_2)_{dB} = 20\log\left(\frac{4\pi r}{\lambda}\right) - 10\log\left(\frac{P_0}{P_r}\right)_{12} \tag{2.3}$$

$$(G_1)_{dB} + (G_3)_{dB} = 20\log\left(\frac{4\pi r}{\lambda}\right) - 10\log\left(\frac{P_0}{P_r}\right)_{13} \tag{2.4}$$

$$(G_2)_{dB} + (G_3)_{dB} = 20\log\left(\frac{4\pi r}{\lambda}\right) - 10\log\left(\frac{P_0}{P_r}\right)_{23} \tag{2.5}$$

From equation (2.3) to (2.5) the gains in dB ($(G_1)_{dB}$, $(G_2)_{dB}$ and $(G_3)_{dB}$) of all the antennas can be determined by simultaneously solving the equations, where r is the distance between the two antennas, λ the wavelength, P_0 is the transmit power and P_r the receive power and thus $\frac{P_0}{P_r}$ the measured power ratio between the two antennas.

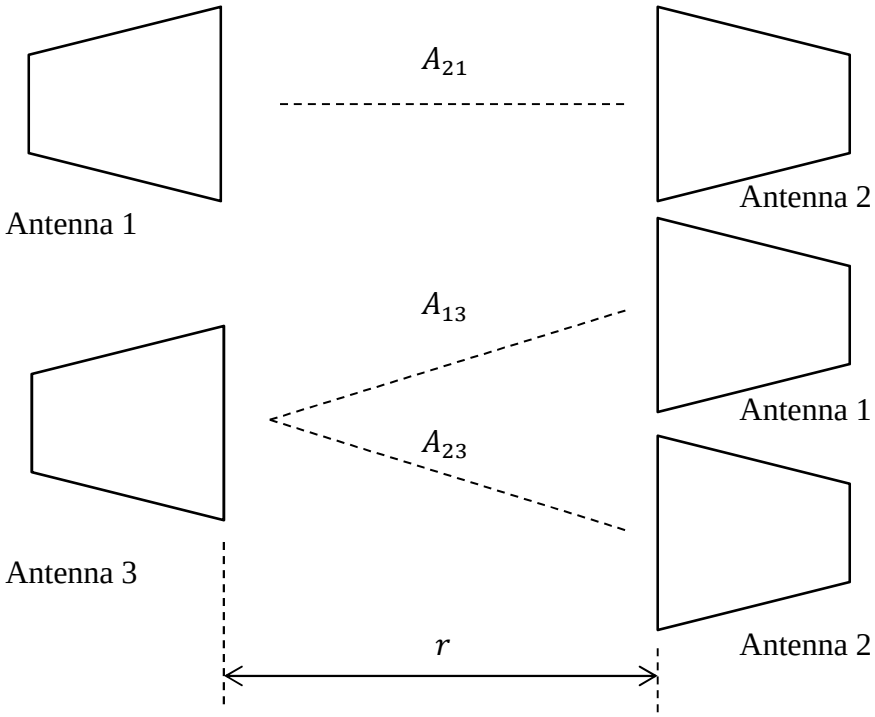

Figure 2.2. Three antenna method [17].

2.2.3. Gain-transfer method

The gain-transfer method is used when an unknown gain of a test antenna is measured by comparing it to a standard gain antenna [26]. These measurements can be performed in either a free space or ground reflection range. Figure 2.3 shows a typical measurement setup inside a CATR, which is a type of free space measurement range. A CATR effectively has a very large reflector antenna which is designed to optimise the planar characteristics of a field in the near-field of the aperture [27]. The CATR used in this dissertation has a parabolic reflector. The source antenna feeds the spherical waves onto the parabolic reflector and converts the waves into plane waves. When the feed is placed at the prime focus of the parabolic reflector, all the waves reflected has travelled the same distance and thus have a uniform phase, for example a plane wave. The usable portions in such test ranges, called the “quiet zone” which is typically about 50% to 60% of the dimensions of the main reflector [27]. The plane wave inside the quiet zone is often a very good approximation of a plane wave but not ‘perfect’. The test antenna is illuminated by a plane wave and the power received into a matched load is measured, then the test antenna

is replaced by the standard gain antenna. Keeping all other conditions the same the received powers are measured again and from the Friis transmission formula the gain of the test antenna can be determined by

$$(G_T)_{dB} = (G_S)_{dB} + 10\log\frac{P_T}{P_S}, \tag{2.6}$$

where $(G_S)_{dB}$ is the power gain of the standard antenna, P_T the power received by the test antenna and P_S the power received by the standard-gain antenna.

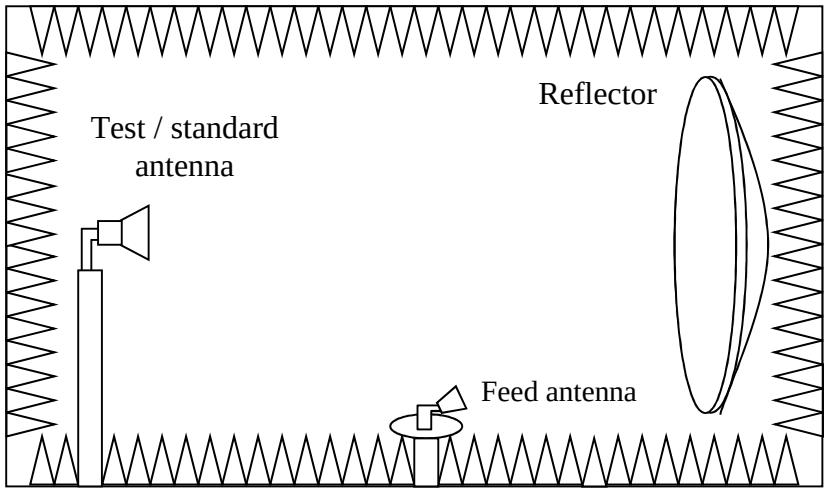

Figure 2.3. Measurement setup in a compact antenna test range.

2.3. COMPLEX ANTENNA FACTOR AND COMPLEX ANTENNA TRANSFER FUNCTION

The next two subsections give some background on the definition of complex antenna factor (CAF) and complex antenna transfer function (CATF) of antennas. Historically, antennas have only been characterised in terms of scalar parameters [19] e.g. antenna gain or antenna factor (AF). Later the complex characterisation of antennas was investigated and the concept of CAF was introduced. An alternative complex characterisation of an antenna is the CATF which was introduced because the general electrical properties of an antenna, e.g. radiation pattern, gain, effective area are not suitable for UWB applications

[1]. For wider bandwidths the parameters are very dependent on frequency and cannot provide sufficient information to characterise UWB antennas.

2.3.1. Complex antenna factor (CAF)

The scalar AF is a well-known parameter for characterising antennas [17]. The CAF includes the phase values in addition to the scalar AF [17]. Figure 2.4 gives a visual presentation of the inputs required to determine the CAF (the coupling circuit can be a matching network or balun).

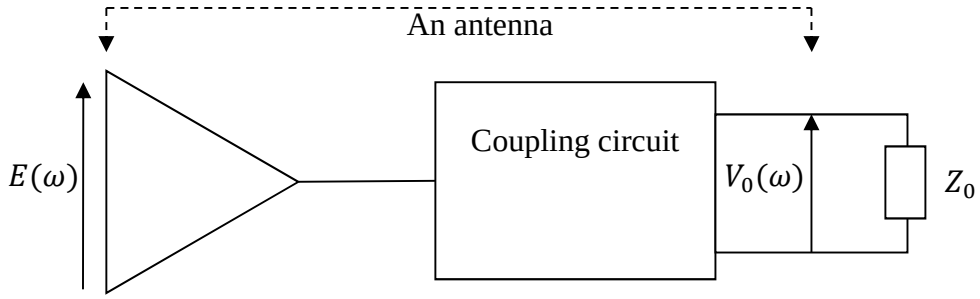

Figure 2.4. Definition of CAF [17].

The CAF is defined by

$$\bar{F}_c(\omega) = \frac{\bar{E}(\omega)}{\bar{V}_0(\omega)}, \tag{2.7}$$

where $\bar{E}(\omega)$ is the electric field of an incident uniform plane wave and $\bar{V}_0(\omega)$ the complex voltage that is generated between the terminals of the load connected to the antenna.

2.3.2. Complex antenna transfer function (CATF)

If two identical antennas are used, the CATF of an antenna [1, 20] can be calculated by using the following equation:

$$\bar{H}(\omega) = \sqrt{\frac{2\pi r_{21} c_0}{j\omega} \bar{S}_{21}(\omega) e^{+j\omega r_{21}/c_0}} \tag{2.8}$$

where ω is the angular frequency, r_{21} the distance between the two antennas, c_0 the speed of light and $\bar{S}_{21}(\omega)$ the measured or calculated complex transmission coefficient between the two antennas.

If CATF of an antenna needs to be determined through measurement and two identical antennas are not available, a reference antenna for which the CATF is known is needed. The CATF of the unknown antenna under test (AUT) can then be determined by using the two antenna method and the following equation from [1]:

$$\bar{H}_{AUT}(\omega) = \frac{\bar{S}_{21}(\omega)}{\bar{H}_{ref}(\omega)} \frac{2\pi r_{21} c_0}{j\omega} e^{+j\omega r_{21}/c_0}, \tag{2.9}$$

where $\bar{H}_{ref}(\omega)$ is the CATF of the known antenna, ω is the angular frequency, r_{21} the distance between the two antennas, c_0 the speed of light and $\bar{S}_{21}(\omega)$ the measured complex transmission coefficient between the two antennas.

A CATF for an antenna (in the frequency domain) can be transformed into an impulse response in the time domain, using the discrete inverse Fourier transform. If the complex transfer function was obtained at discrete frequencies with the resolution $\Delta\omega = 2\pi\Delta f$, the transformation to the time domain needs to be scaled with the appropriate scale factor, $1/N\Delta t$ [1]:

$$\bar{h}^{+}_{n,AUT}(k\Delta t) = \frac{1}{N\Delta t} \sum_{n=0}^{N-1} \bar{H}^{+}_{n,AUT}(n\Delta f) e^{j\frac{2\pi}{N}kn} \tag{2.10}$$

2.4. LITERATURE SURVEY ON CAF/CATF DETERMINATION USING FREQUENCY OR TIME DOMAIN MEASUREMENTS

Frequency domain measurements are often used to determine the CATF of antennas. Different researchers use slightly different approaches in the procedures they follow. ABCD-parameters have been used to determine the CATF, and another innovative approach was to use channel modelling to characterise transfer functions of the receiving antenna, the channel and the transmitting antenna. The CATF of different kinds of antennas were published in [1, 3, 20, 21] using the two identical antenna method and measuring the S_{21}-parameters. There are two different ways to determine the CATF, either by using measurements in the frequency domain, or measurements in the time domain, this will be discussed further in this section.

The authors of [4, 7] thought it best to use the ABCD-parameters to determine the CATF of the receive antenna and the transmit antenna. The transmission coefficient was measured between two identical Vivaldi antennas in an anechoic chamber [7]. Results were compared [7] to simulations, but no results were shown as direct comparison between the simulated and measured data. They did however state in their conclusion that the results did compare well. No further literature was found on using the ABCD-parameters to determine the CAF or CATF. By using this approach it seems like there is an extra (unnecessary) step included in the procedure to determine the CAF or CATF of an antenna.

The channel modelling approach was used by authors [5, 8 – 12] to determine the transfer function of both the transmitting and the receiving antenna. The approach taken was to break the system into different parts, analyse it, and then to combine all the parts again to calculate the transfer functions of the antennas.

Figure 2.5 shows a schematic of how the antennas were used in [5], with the transmit antenna and the channel (free space) viewed as one part and the receive antenna as another part.

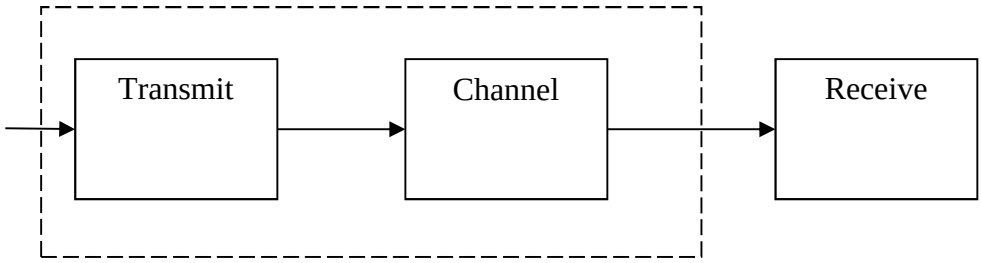

Figure 2.5. Measurement system: Transmit and channel as one section and receive antenna as another.

From the discussions in [5] one can assume that the phase response was measured, but no final results for the phase were presented in the paper. The authors did however perform measurements with the antennas positioned at different angles from one another, and determined the group delay and gain variations at these different angles.

In [9 – 11] the approach to obtain transfer functions was to look at each component in the system separately - see Figure 2.6. The components in the system are the transmit antenna, the channel and the receive antenna.

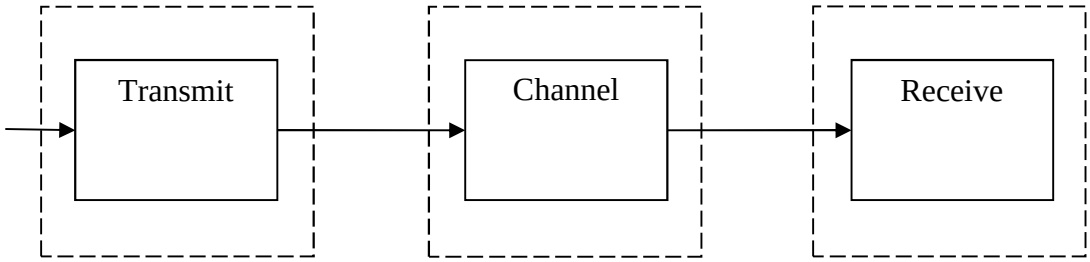

Figure 2.6. Measurement system: Three sub-sections considered

A transfer function was determined for each separate component. In [10] measurements were performed in the frequency domain using compact band-reject U-slotted planar antennas. The CATF ($\bar{H}(\omega)$) was determined for each antenna, at different antenna orientations relative to each other. This model allows the transmit- and the receive- antenna to be separated entirely from the free space channel. The impulse responses, determined from the CATF of the antenna at different angles, indicated that this model can be used for

mixed signal modelling [9]. In [10] and [11], continuing from [9] directional transfer functions were determined for the U-slot antenna. The characterisation for the U-slotted antenna was done using different waveform excitations and antenna orientations, which allow designing and optimisation of a transceiver antenna for UWB applications.

The previously published literature summarised in this section primarily focused on the magnitude of the CATF and the directional impulse responses of the antennas, and not so much on the phase response.

A number of studies on CAF were done for dipole antennas. The authors of [14 – 19] focused on the measurement of dipoles with baluns. A balun connects a balanced line, e.g. a dipole, to an unbalanced transmission line e.g. a coaxial transmission line. It was necessary to determine the transmission characteristics of the balun first before the CAF of the dipole antenna could be determined.

The authors of [17, 18] first determined the CAF in the near field and then converted it to the far-field region. This was done because the dipoles needed to be placed far apart to be in the far-field and when doing that other factors such as the ambient reflection and external noise can possibly influence the measurements. Measurements were performed on monopoles and dipoles, and baluns were used – the effect of these baluns had to be incorporated in the calculations. The CAF of the baluns and antennas were also determined for each case.

In [16] the CAF of a V-dipole was determined using the three antenna method. Using the result of the three antenna method, the gain-transfer method was used to determine the CAF of an unknown V-dipole with a balun. (The three antenna method produced less accurate phase response than the two antenna method, where two identical antennas are used. This is because the distance between the antennas could not be determined accurately which introduced more errors into the final result, due to more antennas involved in the measurement method.

In [22] the three antenna method was used to determine the transfer function of a double ridge guide horn antenna. Pattern descriptors e.g., energy gain, correlation coefficient and correlated energy were determined.

In the papers discussed earlier, the transfer function is dependent on the distance r between the two antennas. The distance r has a large effect on the phase response - hence it is very important to use the correct distance between the antennas. The authors in [21] gave detail on a number of different methods that can be used to determine the distance accurately.

Time domain measurements are performed by using a high frequency oscilloscope and a short pulse generator [3, 5]. The pulse is transmitted through the transmit antenna and captured by the receive antenna. According to [2] the phase information could not be obtained from the time domain measurements they performed and thus the inverse Fourier transform from frequency domain measurements were required.

The main advantage of using the frequency domain to determine the CATF, is that the transmission coefficient can be easily measured with a VNA. A VNA has well established standardised calibration techniques available, to eliminate the effects of the cables in the system and has a typical dynamic range of 90 dB. The complex transmission coefficient can easily be stored on the VNA and used in calculations.

Time domain characterisation is not as well established as frequency domain characterisation. In the frequency domain the VNA can be calibrated, standard methods are available and data can be easily captured.

The main disadvantages of determining the CATF in the time domain are that narrow pulses and ultrafast scopes are required to perform the measurement. It is difficult, using this method, to determine all the components that may interfere with the measurement and then try to eliminate the effects to obtain the actual result or transfer function in the time domain. The phase information cannot be easily extracted, and needs to be measured in the frequency domain and then the inverse Fourier transform is utilised to obtain the phase information in the time domain.

2.5. SUMMARY

Background information on various aspects relevant to the topic of this dissertation have been presented in this chapter. The different measurement methods available to measure antenna radiation parameters have been summarised and definitions given for CAF and CATF. A summary of previous research related to the determination of CAF and CATF using frequency or time domain measurements was presented.

The aim of this dissertation is to determine the CATF of an ultra-wideband (UWB) antenna using frequency domain measurements – the antenna can then be used as UWB measurement standard in a CATR. Frequency domain measurements were chosen because a VNA was readily available and easy to calibrate.

CHAPTER 3 CHARACTERISATION OF A DRGH ANTENNA

3.1. INTRODUCTION

As mentioned previously one of the objectives of this dissertation is to characterise a 1-18 GHz Double ridge guide horn (DRGH) antenna by obtaining its complex antenna transfer function (CATF). In order to achieve this experimentally two identical DRGH antennas were accurately measured in an anechoic chamber. To ensure the necessary accuracy of the measurements, care has to be taken with the measurement setup. The setup and calibration technique required needed to perform accurate and reliable measurements are discussed in detail in this chapter, and the results of the measurements are presented. A numerical model was also set up for the antenna and simulations performed using a full-wave electromagnetic analysis software package called FEKO. The simulated CATF acts as validation for the experimental results. Also presented in this chapter is an illustration that the CATF of an unknown antenna can be experimentally determined in an anechoic chamber if you have at your disposal an antenna with a known CATF.

Section 3.2 broadly outlines how the CATF of the DRGH antenna was determined from measurements. In Section 3.3 the setup of the numerical model of the 1-18 GHz DRGH antenna in FEKO is presented. Section 3.4 discusses the experimental measurement setup, including the calibrations and measurements required to determine the CATF of the antenna. In Section 3.5 the measured and simulated results of two identical antennas are compared. Additional measurements were also performed in an anechoic chamber with two different antennas (described in Section 3.6), using a standard antenna as well as an AUT. For each AUT, an identical antenna was available and could validate the CATF. The chapter is finally concluded with a short summary in Section 3.7.

3.2. CATR OF A DRGH ANTENNA USING THE TWO ANTENNA MEASUREMENT METHOD

3.2.1. Procedure for determining the CATF in an anechoic chamber

The two antenna measurement technique was used to measure two identical DRGH antennas – with the aim to calculate the CATF of the antennas. The measurements performed for this dissertation was similar to that in [1, 20] and the CATF can be determined using equation (2.8) in Chapter 2 of this dissertation. The transmission coefficient between the two antennas was measured in the far-field region of the antennas. The distance between the two antennas, r_{21}, was chosen to satisfy the general requirement to be in the far-field region:

$$r_{21} > \frac{2D^2}{\lambda}, \tag{3.1}$$

where D is the maximum aperture dimension of the antenna and λ is the wavelength at which the antenna operates. DRGH antennas characterised in this dissertation operate in the frequency band of 1-18 GHz. The antennas used in this dissertation had a maximum aperture dimension of 0.25 m for the largest antenna - the antennas were placed at least 8 meters apart to ensure that the measurements and simulations are performed well inside the far-field region.

Once the CATF of the identical antennas was obtained, it could then be used as reference to determine the CATF of other unknown antennas. This reference antenna can also be seen as a CATF standard antenna. Equation (2.9) in Chapter 2 can be used to determine the CATF of an unknown antenna after a transmission measurement is performed between the unknown and standard antennas in the anechoic chamber, again making sure that the distance between the antennas is such that far-field operation can be assumed.

3.2.2. Phase un-wrapping

Reference [1] discusses proper phase un-wrapping of the calculated CATF of an antenna. A meaningful answer can only be obtained from equation (2.8) if the phase results (the square root allows for two possibilities) are interpreted the correct way. By drawing the two phase responses against frequency, see Figure 3.1 (response 1 and response 2), the unwrapping can be clearly seen (Unwrapped phase). One can see that from the two answers, to avoid discontinuation in the phase results, part of the one response and part of the second response are used to obtain the final result. The actual answer would be a combination of the two as indicated in Figure 3.1. This phase un-wrapping was required for all the measurements where two identical antennas were involved.

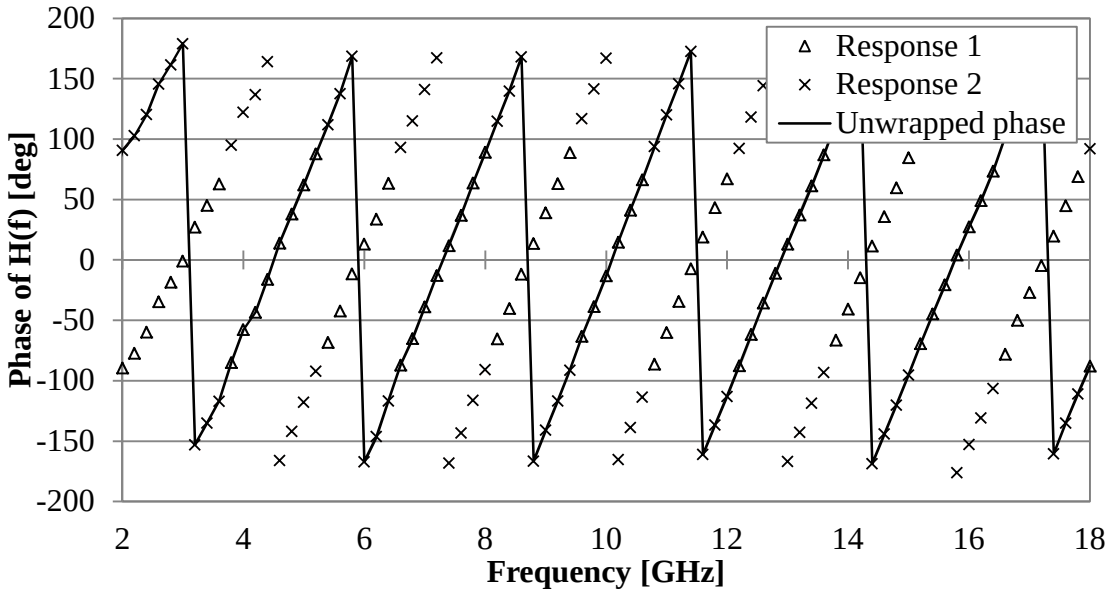

Figure 3.1. Selecting the correct phase results.

3.2.3. Antenna detail

Four antennas were characterised in the dissertation. Table 3.1 lists the antennas that were used and for which the CATF's were calculated. Figure 3.2 shows photographs of the antennas listed in Table 3.1.

Table 3.1. Antenna detail

Antenna identification	Model	Part Number	Serial number	Frequency range measured [GHz]
SAAB1	ETS-Lindgren	3115	00069438	1 – 18
SAAB2	SAAB EDS.	470532-00000	08033001	1 – 18
EDS1	SAAB EDS.	470549-00000	10093001	1 – 18
EDS2	UP	-	10113001	1 – 18

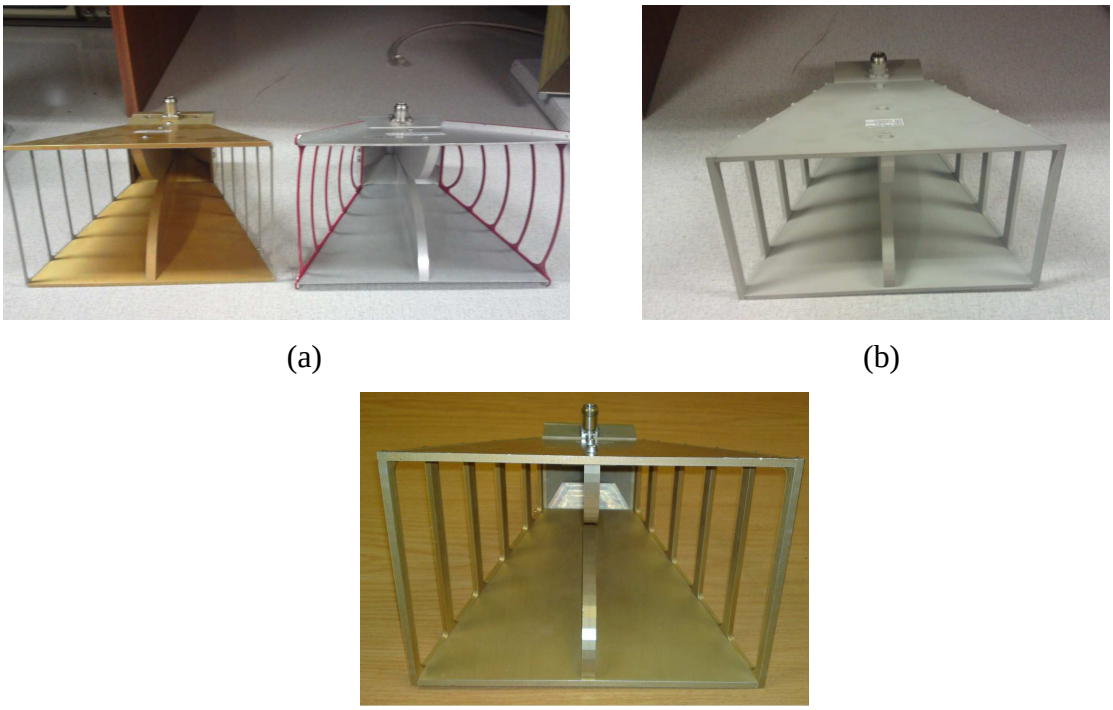

(a) (b)

(c)

Figure 3.2. Antennas used for measurements a) SAAB1 and SAAB2, b) EDS1 and c) EDS2.

3.3. FEKO SIMULATION TO DETERMINE THE CATR

3.3.1. Numerical solver and calculations

Complex electromagnetic radiating structures can easily be analysed by using FEKO [24], which utilises advanced numerical methods to perform full-wave electromagnetic analyses. Antennas of many different types (including DRGH antennas) can be analysed to accurately obtain various antenna parameters e.g. reflection coefficient, radiation patterns, gain, etc.

Octave [28] and MatLab [29] are programming software packages that are intended for numerical computations, and have good matrix manipulation capabilities. Octave, a free alternative to MatLab, was deemed suitable for this application and has the necessary computational power to calculate the CATF from the measured or simulated antenna characteristics. A large number of data points, over the frequency range 1 – 18 GHz, were used in the simulations to determine the CATF of the antennas. Complicated mathematical calculations involving large matrices needed to be solved to calculate the CATF.

3.3.2. FEKO model

The DRGH antennas were modelled in FEKO by B. Jacobs [23]. Those models were configured to have two of the same antennas placed in the far-field region from each other. The transmission coefficient was obtained through simulation and, by using equation (2.8) the CATF of the two identical antennas was calculated.

The antennas modelled in FEKO are a very good representation of the physical antennas. The physical antennas and the modelled antennas both ended in female Type-N connectors. One antenna was excited with 1 V at the input port. The complex $\bar{S}_{21}$ parameter was obtained - port 1 is associated with the first antenna and port 2 associated with the second antenna. The antennas were horizontally aligned and were spaced a distance of 8 m apart, with the centre of the one antenna opposite the centre of the other

antenna. The distance between the two antennas was measured from the one aperture to another. This distance is important for the calculation of the CATF.

The results of the FEKO simulations are used in Section 3.5 to compare to the results obtained with the experimental data, for validation purposes.

3.4. DETAILS OF EXPERIMENTAL MEASUREMENTS TO DETERMINE THE CATF

Experimental measurements were performed in an anechoic chamber using two identical 1 - 18 GHz DRGH antennas. The antennas were placed in an anechoic chamber at the same height and levelled, vertically and horizontally, facing each other - exactly the same setup as in the FEKO simulations. The antennas were placed approximately 8 meters apart to be in the far-field region.

An attempt was made to measure the distance between the two antennas with a measuring tape, but it was very difficult measure it accurately, because of the antennas being so far apart. The 8510C vector network analyser (VNA) was then used to determine the distance between the antennas by performing a time delay measurement between the two antennas, measured from antenna connector to another. A correction to this distance needed to be applied to get the distance from one aperture to another. These time domain measurements were assumed to be more accurate than the measurements with the tape measure. The VNA was used to measure the complex transmission coefficient, $\bar{S}_{21}$, between the two antennas in the frequency domain.

A number of challenges were faced during the experimental measurements, due to limited equipment available at the facility. These challenges and solutions are discussed in the sections to follow, and the process followed to obtain the CATF of the DRGH antennas.

3.4.1. VNA calibration

To measure accurately, the VNA needs to be calibrated to eliminate the effects of the cables and connectors that were used in the measurement setup. The VNA must be calibrated in such a way that only the antennas are measured and nothing else.

The VNA was set up, using Sucoflex type SF 106 RF cables, that ends in a 3.5 mm connector. The Sucoflex cables are high performance flexible microwave cables, which were long enough so that the antennas could be placed in the far-field of one another and still give good performance. The Type-N cables that were available showed high losses and was not deemed suitable. The VNA was calibrated using an 85052B (3.5 mm) calibration kit, which includes sliding loads for the calibration above 2 GHz. The sliding loads provide a better correction of the directivity, to give more accurate measurements of the voltage reflection coefficient (VRC).

Adapters were required (3.5 mm or SMA to Type-N) for the connection between the cables and the antennas. SMA connectors are compatible to 3.5 mm connectors; it means that the two can be connected together without damaging the connector. SMA connectors are not precision connectors meaning that they have bad repeatability. SMA to Type-N was used because they were the only adapters available at the time of measurement. These adapters were calibrated separately and the correction was applied to the measurement data to compensate for them, see Section 3.4.2.

Both the antennas end in female Type-N connectors and required male connectors to connect to the antennas. As the VNA requires a thru connection as part of a full two-port calibration, these male connectors cannot be connected directly to one another so a special calibration technique was required, an adapter removal technique. The adapter used for the adapter removal technique was a female-female adapter. Two full two-port calibrations were required to complete the calibration so that the adapter can be removed to end up with male connecters that can be connected up to the female connectors of the antennas.

Due to the number of points and the sliding loads, which introduced six extra measurement runs for each port, the calibration was very time consuming. Therefore the configuration

was changed and the calibration at the facility was made faster and easier, but compromising on the uncertainty introduced, due to the extra measurement steps involved that are explained in the next few paragraphs.

At the measurement facility, where the experimental antenna measurements were performed, a Type-N calibration kit was not readily available, so the calibration of the VNA was performed in 3.5 mm connector type. The cables were set up in such a way that the two ports can be connected without performing an adapter removal technique, which saved some time during the experimental measurements. Two adapters, NM (Type-N male) to SMA (Female) and NM to SMA (Male) were then used to connect the cables to the antennas, which were measured separately, see Section 3.4.2. See Figure 3.3 for the illustration of the measurement setup. Figure 3.4 shows the antennas in the anechoic chamber.

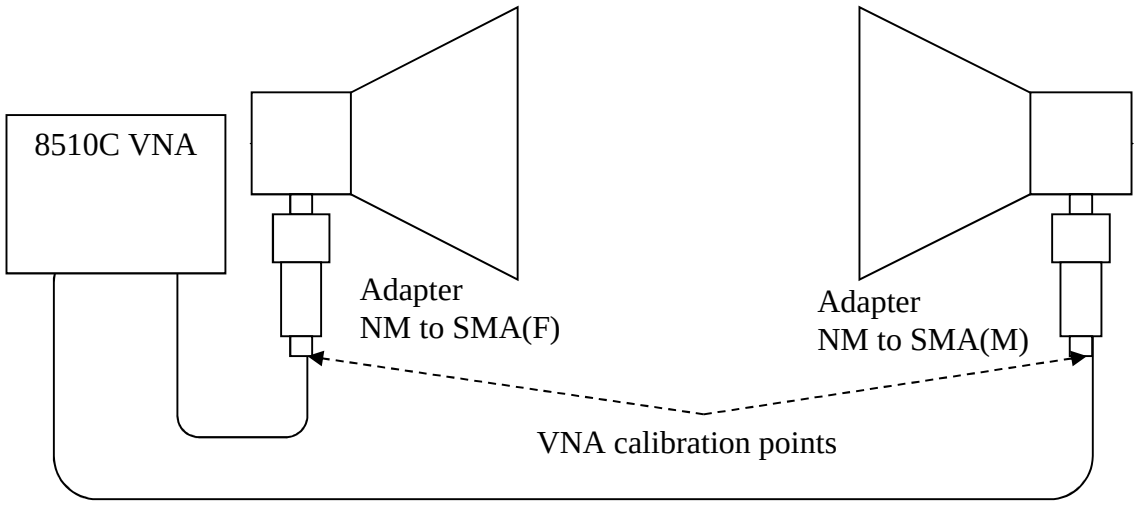

Figure 3.3. Measurement setup for calibration and calibration point of the VNA.

Figure 3.4. Photo of the measurement setup of the antennas in an anechoic chamber.

The VNA calibration was performed in two frequency bands, 1 to 9.5 GHz and 9.5 to 18 GHz. The maximum number of points the 8510C VNA can store, per calibration or measurement, is 801. Over this wide frequency band the phase measurements of the S-parameter changes very fast and therefore required more measurement points over the frequency band, not to lose any information.

Figure 3.5 gives an illustration of the difference between the results, with 201 points and 21 points within the frequency band 5 to 7 GHz. The 21 points in the figure below can give an inaccurate indication of the phase values. A small frequency range was chosen and the number of points was increased until the number of points correctly represented the actual signal.

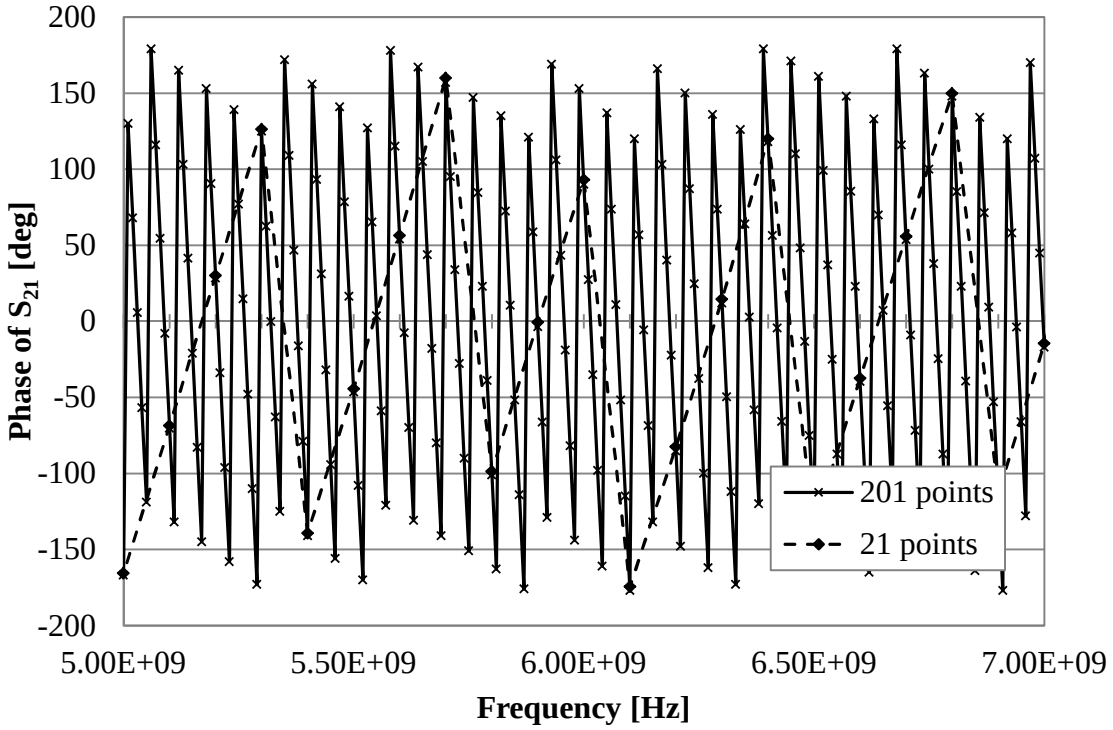

Figure 3.5. Phase of $\bar{S}_{21}$ and the effect of not enough measurement points.

The VNA calibration was now complete, and the transmission and reflection coefficients of antennas were measured. The measurement results, obtained in this measurement step, included the adapters that were connected to the antennas to convert from 3.5 mm to Type N. In order to remove the adapters from the measurement result the adapters needed to be measured separately and a correction has to be applied - details are discussed in Section 3.4.2.

The distance between the antennas was measured in the time domain while the VNA is calibrated for a specific frequency range, more details can be found in Section 3.4.3.

3.4.2. Adapter calibration and correction applied

The adapters used to connect the calibrated cable ends to the female antenna connectors also needed calibration. These results were then used to apply a correction to the measured data. The adapters were also calibrated using a calibrated VNA. The magnitude and the

phase of the transmission coefficient were measured to quantify the correction to be applied to the measurements performed in Section 3.5 and 3.6.

Effectively after applying all the corrections that were introduced by the adapters the new calibration point has moved from before the adapters to after the adapters, as seen in Figure 3.6.

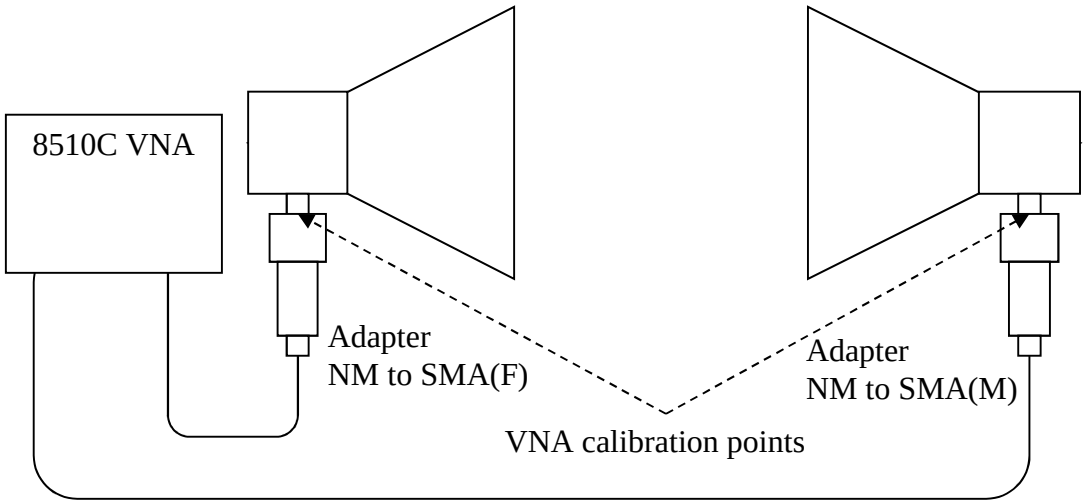

Figure 3.6. Measurement setup for calibration and calibration point of the VNA. Effectively the calibration point was shifted by correcting for the adapters used.

The simplest way to determine the transmission coefficients of the adapters were to connect the two adapters together, as one of the SMA connecters was male and the other female. The other ends of the adapters were both Type-N male connectors. See Figure 3.7 for a visual presentation of the adapter configuration and Figure 3.8 for a photo of the adapters. Due to the two male connectors, which are non-insertable, a full two-port adapter removal technique calibration, over the frequency range, was required.

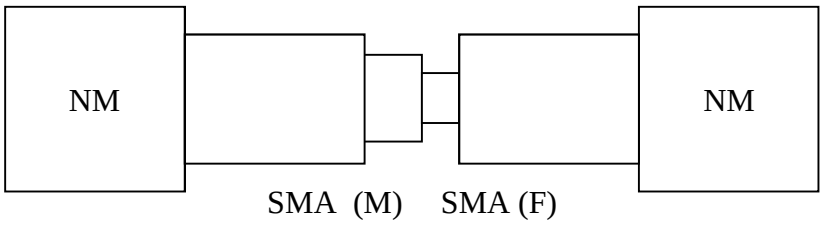

Figure 3.7. Adapter configuration to measure the S_{21}.

Figure 3.8. Type- N (Male) to SMA (Female) and Type- N (Male) to SMA (Male) adapters.

The VNA, an HP8510C, was set up with two cables that ended in female Type-N connectors as can be seen in Figure 3.9. The VNA was calibrated using the adapter removal technique, using a Type-N calibration kit, HP85054B, which included sliding loads as part of the calibration. Although this calibration was time consuming, it only had to be done once and it could be done outside of the anechoic facility as all the measurements were performed in coaxial cable and not free-field. The complex transmission coefficient, $\bar{S}_{21}$, of the adapters were measured. Figure 3.10 shows the VNA used with the adapters connected to the ends of the cables.

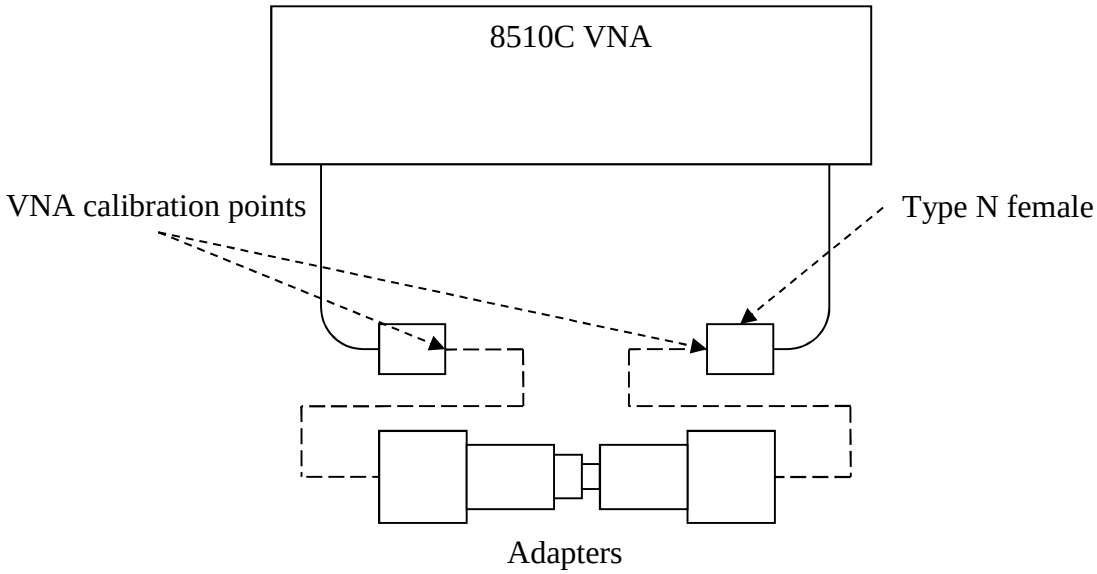

Figure 3.9. VNA setup for the measurement of the adapters.

Figure 3.10. Photograph of the adapters connected to the VNA.

Figure 3.11 and 3.12 give the magnitude and the phase of the transmission coefficient of the adapters, as it was measured on the calibrated VNA. The dB value is simply added to the magnitude of the measured data of the antennas in Section 3.5 and 3.6.

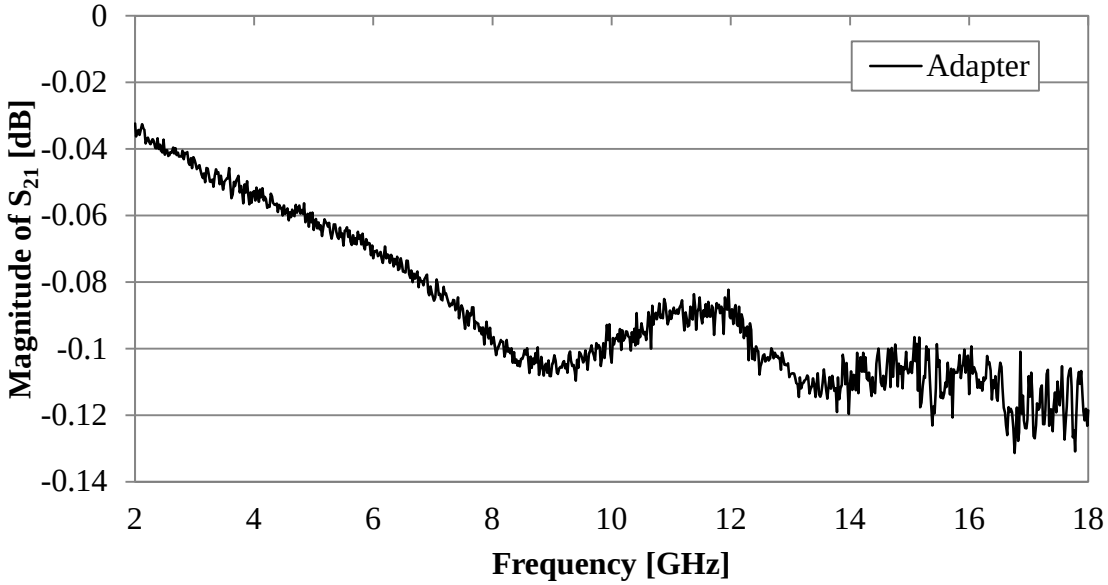

Figure 3.11. Magnitude of $\bar{S}_{21}$ of the two adapters connected to one another.

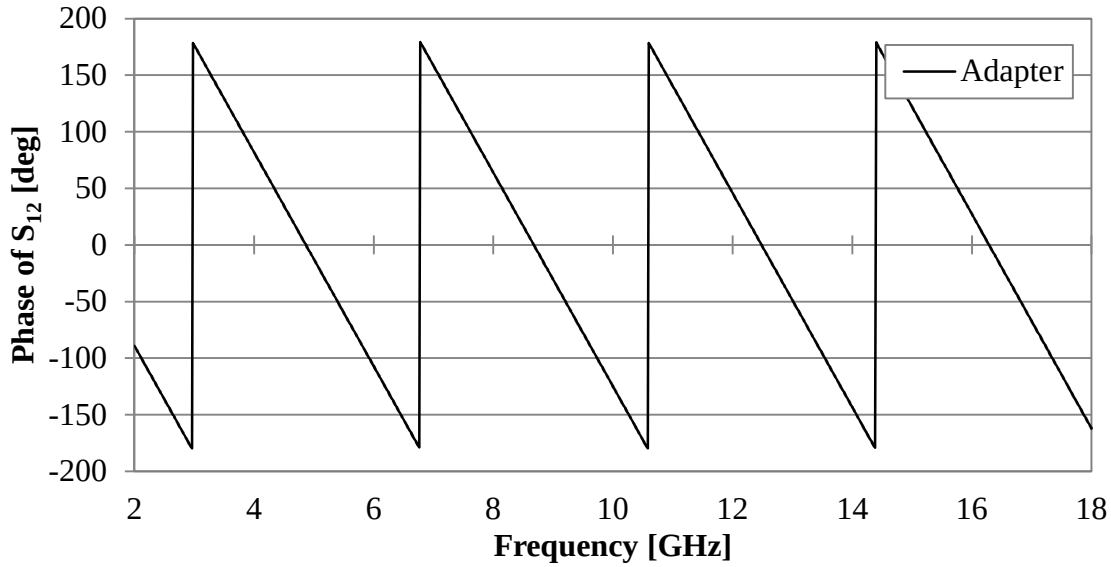

Figure 3.12. Phase of $\bar{S}_{21}$ of the two adapters connected to one another.

In order to make a correction for the phase measurements the complex transmission coefficients were transformed to the time domain where the length of the two adapters could be determined. The time domain was measured to determine the electrical length of these adapters that is used to correct the phase of the CATF of the antennas measured in the anechoic chamber. Figure 3.13 shows the time domain measurement of the adapters. Section 3.4.3 gives detail on the calculations and correction that need to be applied for the distance between the two antennas.

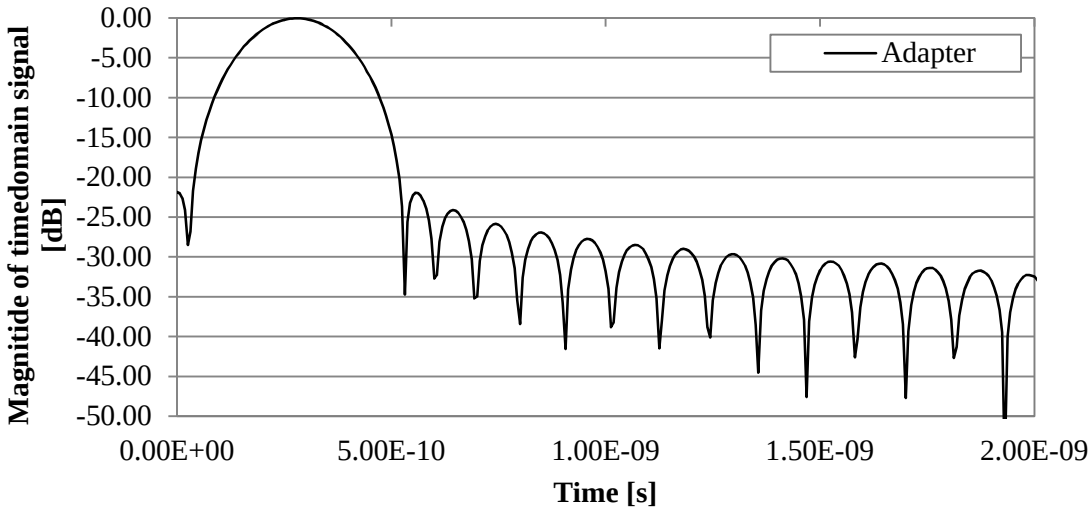

Figure 3.13. Time domain measurement of the adapters

3.4.3. Time domain measurements to determine distance

The time domain measurements were used to determine the distance between the two antennas. The distance r_{21} is required to determine the CATF of the antenna using equation (2.8) in Section 2.3.2. The time delay measured in the time domain was necessary as it was very difficult to accurately measure the distance between the two antennas, using a measuring tape. The time domain measurement gives a delay that can be converted to a distance.

For each of the transmission coefficient measurements performed, between two antennas, the time delay in the time domain was also measured. The distance,

$$r_{anechoic} = t \times c_0, \tag{3.2}$$

was calculated using the measured time delay, t, and the speed of light c_0. The delay measured by the VNA is the delay between the two calibration points, which also included the two adapters.

Figure 3.14 shows a typical time domain measurement that was used to determine the distance, from port to port, between the antennas. The average of the maximum of

measurement 1 and measurement 2 in Figure 3.14 was used as the time delay measurement and was then converted to the distance, $r_{anechoic}$.

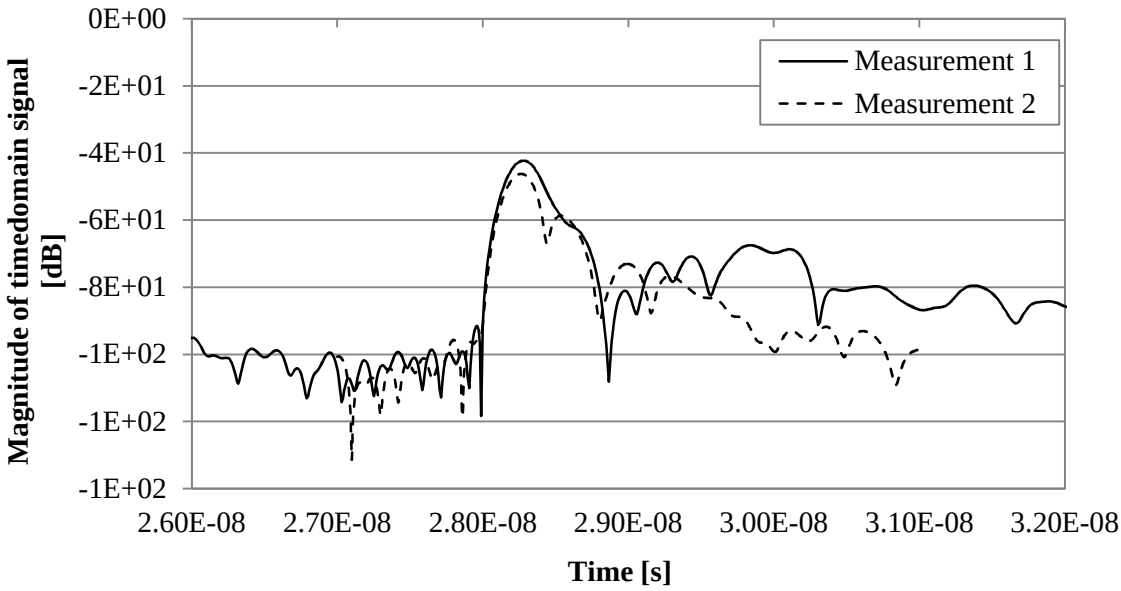

Figure 3.14. Example of time domain measurement to obtain $r_{anechoic}$, measurement 1 is from 1 to 9.5 GHz and measurement 2 is from 9.5 to 18 GHz.

For each set of antenna measurements performed in Section 3.5 and 3.6, the time delay in the time domain was measured to determine the distance between the antennas. In Section 3.4.2 the time delay of the adapters was determined. The antenna length also had to be subtracted as $r_{21}$is defined as the distance between the two antenna apertures. Equation (3.2) was used to calculated the distances. The distance used in the CATF calculations is

$$r_{21} = r_{anechoic} - 2r_{adapter} - r_{antenna\ length,A} - r_{antenna\ length,B}, \quad (3.3)$$

where, $r_{anechoic}$ is the distance obtained when the antennas were measured in the anechoic chamber and $r_{adapter}$ the distance obtained when the adapter were measured. $r_{antenna\ length,A}$ and $r_{antenna\ length,B}$ are the antenna length measurements from the antenna port to the aperture for the different antennas.

3.4.4. Transmission coefficient measurements between antennas

The transmission coefficients of the antennas were measured for different combinations of antennas. Table 3.2 gives the summary of the antennas measured, with the frequency range.

Table 3.2. Antennas measured in anechoic chamber.

Identifier	Antenna 1 Serial number	Antenna 2 Serial number	Frequency range [GHz]
EDS1-EDS2	10093001	10113001	1 to 18
EDS1-SAAB1	10093001	00069438	1 to 18
EDS1-SAAB2	10093001	08033001	1 to 18
EDS2-SAAB1	10113001	00069438	1 to 18
SAAB1-SAAB1	08033001	00069438	1 to 18
EDS1-SAAB2	10113001	08033001	1 to 18

The transmission coefficient, $\bar{S}_{21}$, between antenna EDS1 and EDS2 is displayed in Figure 3.15 to 3.16. For illustration purposes, the phase response of the transmission coefficient is only displayed for a 2 GHz bandwidth. Here one can see that the phase changes rapidly and this is why a large number of points were required for the measurements.

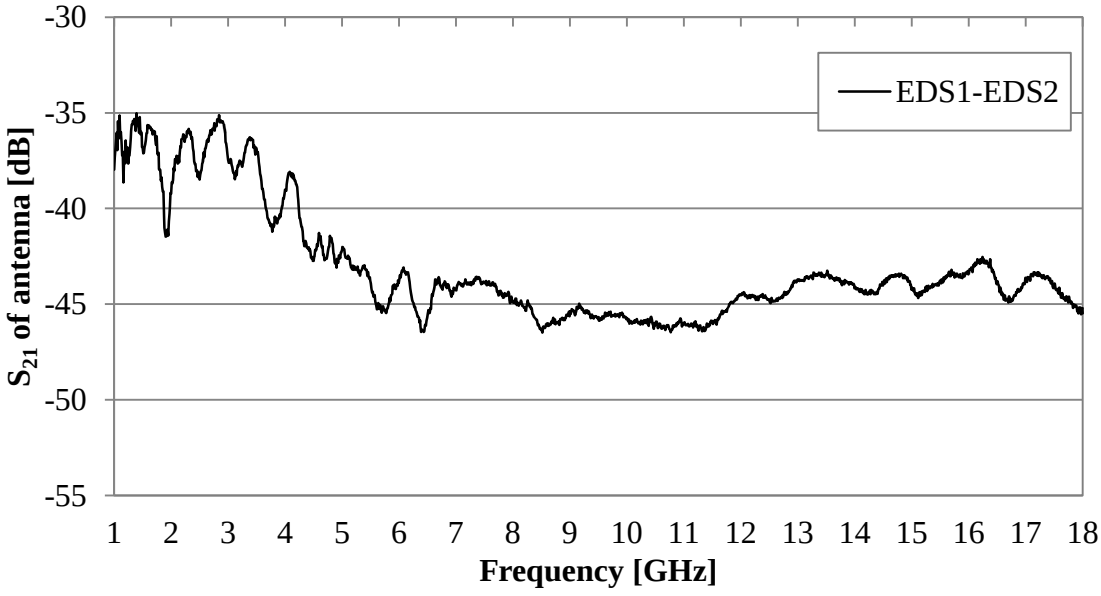

Figure 3.15. Magnitude of $\bar{S}_{21}$ between EDS1 and EDS2.

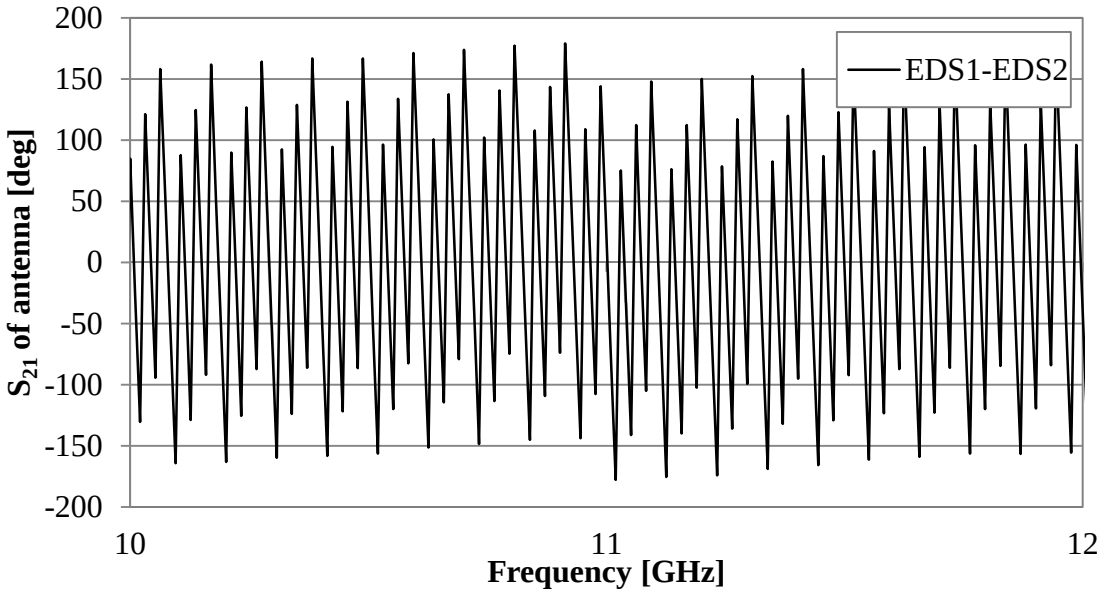

Figure 3.16. Phase of $\bar{S}_{21}$ between EDS1 and EDS2.

3.5. COMPARISON OF SIMULATED AND MEASURED RESULTS

In this section the CATF are determined using the antenna measurements described in Section 3.4.4. The results are validated with simulations performed using FEKO.

Assuming two identical antennas, equation (2.8) are used to determine the CATF of the antennas. Figures 3.17 and 3.18 show the CATF of the DRGH antenna EDS1 (sn 10093001) and EDS2 (sn 10113001) measured in the anechoic chamber and also the simulated results using FEKO.

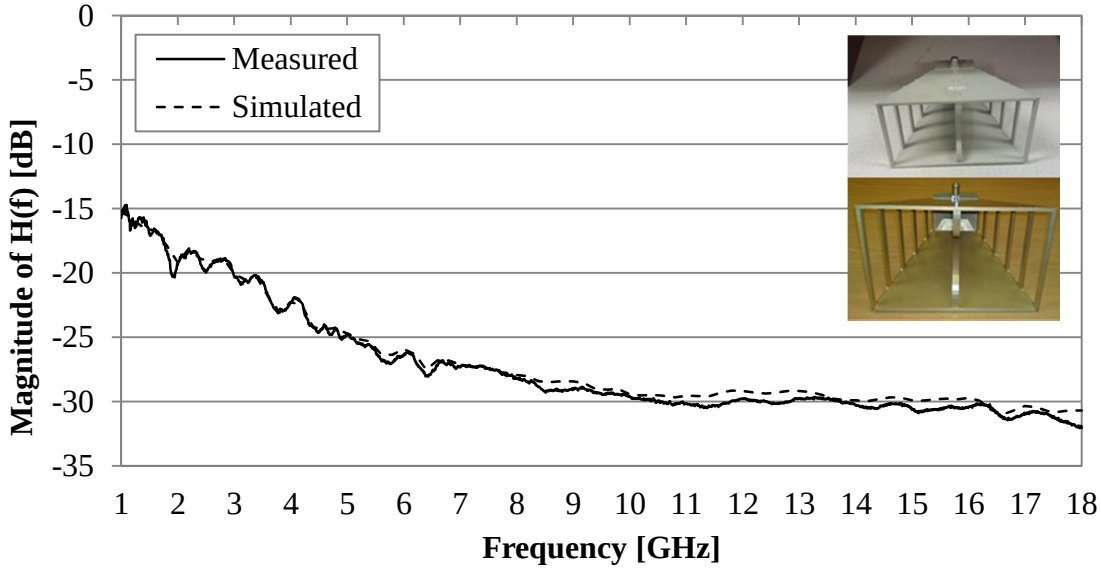

Figure 3.17. Magnitude of CATF for identical antennas EDS1 and EDS2.

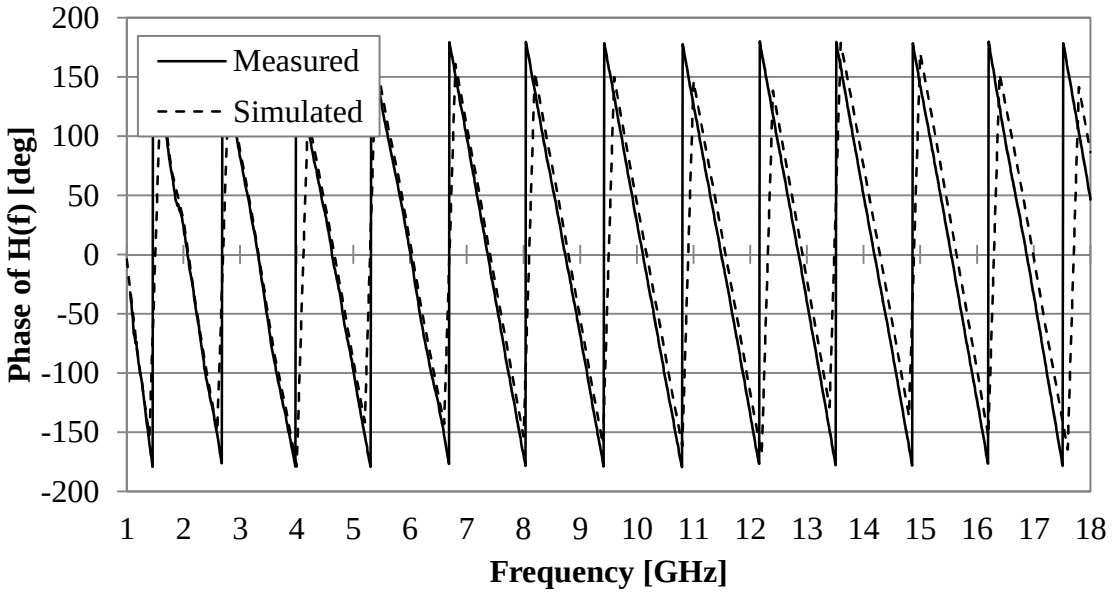

Figure 3.18. Phase of CATF for identical antennas EDS1 and EDS2.

Figure 3.19 and 3.20 show the CATF magnitude and phase of identical antennas SAAB1 (sn 00069438) and SAAB2 (sn 08033001). These results also compare well with the FEKO simulated results of this antenna.

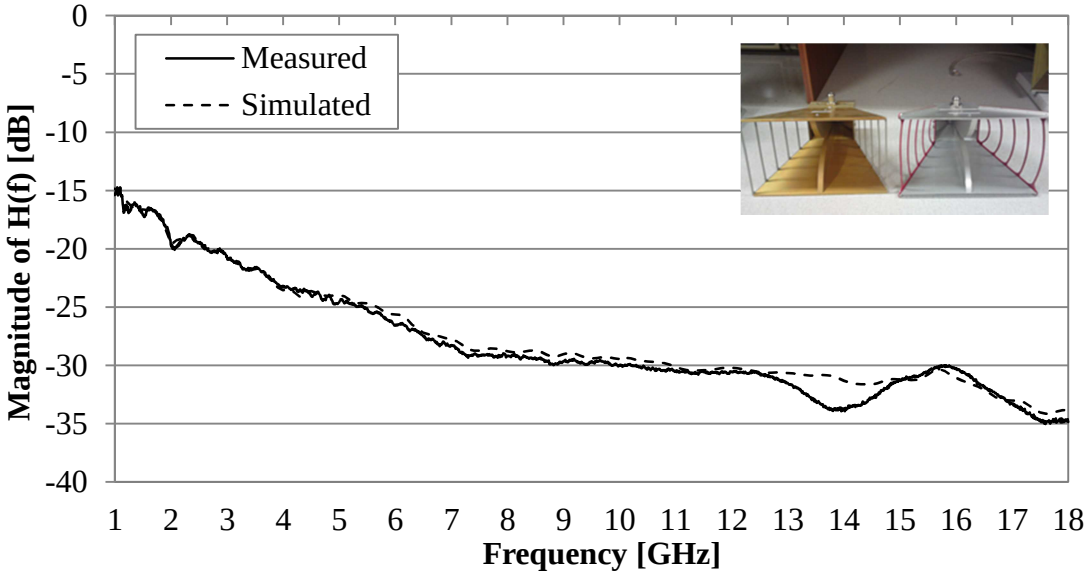

Figure 3.19. Magnitude of CATF for identical antennas SAAB1 and SAAB2.

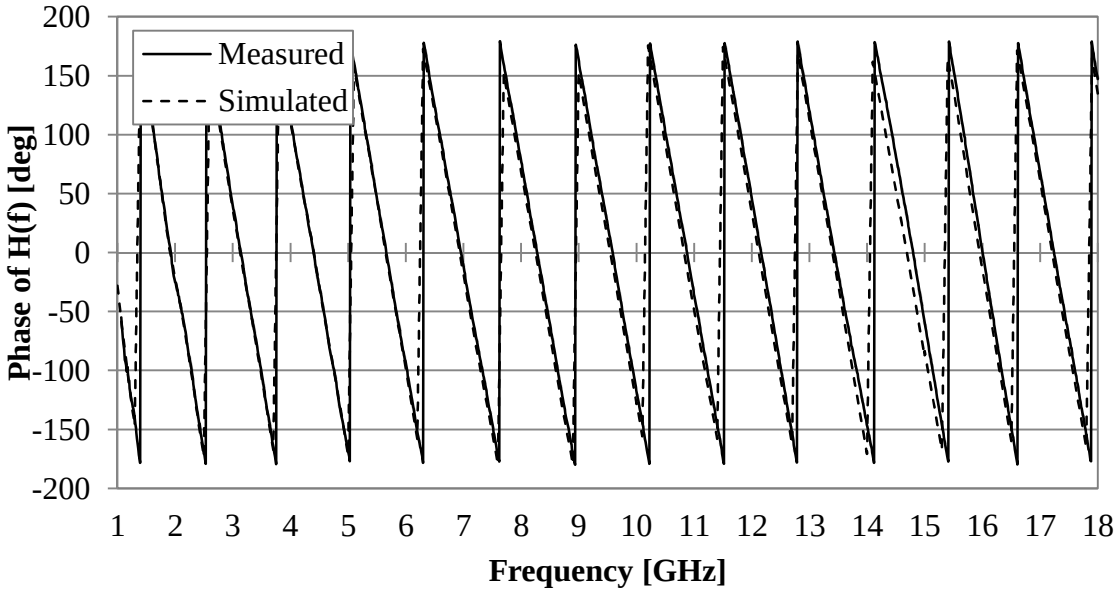

Figure 3.20. Phase of CATF for identical antennas SAAB1 and SAAB2.

The CATF of different antennas were determined through measurements and simulations – the results agreed very well (magnitude and phase), confirming that the measurement method are valid and the CATF of antennas can be determined in an anechoic chamber.

3.6. VERIFICATION THAT THE CATF OF AN UNKNOWN ANTENNA CAN BE DETERMINED IN ANECHOIC CHAMBER USING A CATF STANDARD ANTENNA

The aim of this section is to illustrate that the CATF of an unknown antenna can be determined from measurements in an anechoic chamber using a standard CATF antenna (an antenna for which the CATF is known already). The same antennas and measurements as listed in Table 3.2 were used for this illustration.

For the first example the two identical antennas measured in the anechoic chamber, EDS1 and EDS2, with sn 10093001 and sn 10113001, was used as the CATF standard antenna. Equation (2.8) was then used to calculate $\bar{H}(f)$ of the unknown antenna SAAB2, with sn 08033001. The magnitude and phase results of this antenna were compared to the measured results of the two identical antennas SAAB1 and SAAB2, and also to the simulated results obtained from FEKO. The results (which are presented in Figure 3.21 and 3.22) compare very well.

As a second example the SAAB1 was used as the CATF standard antenna, and the CATF of antenna EDS1 was determined, using equation (2.9). The magnitude and phase of the CATF of the SAAB1 antenna are compared in Figures 3.23 and 3.24 respectively, again showing good correlation between the three sets of results.

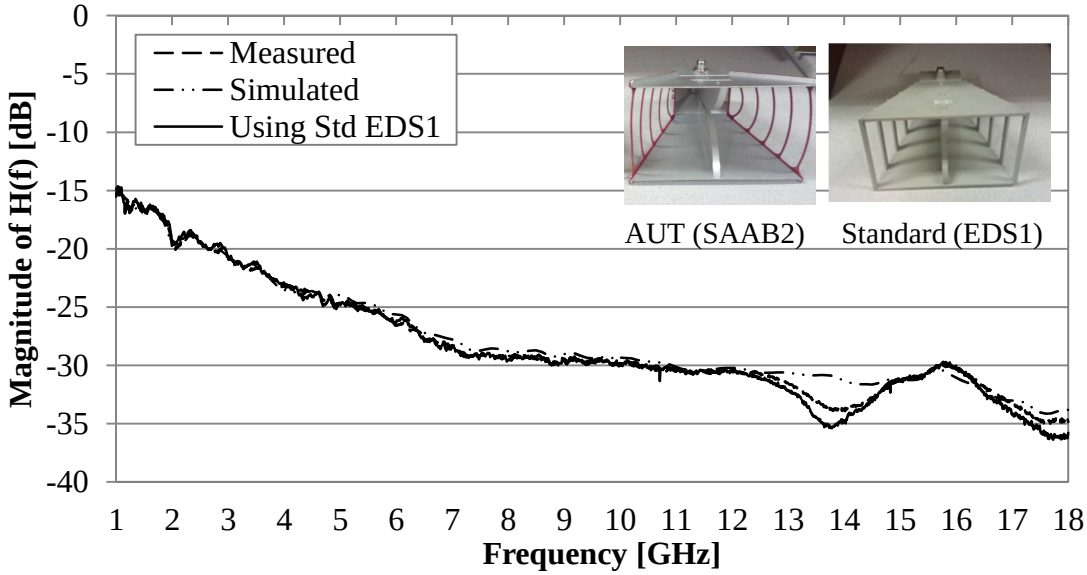

Figure 3.21. Comparison of the magnitude of CATF for SAAB2 obtained using three different approaches; two identical antenna measurement technique, two identical antenna simulations in FEKO, and two antenna measurement technique using CATF standard antenna EDS1.

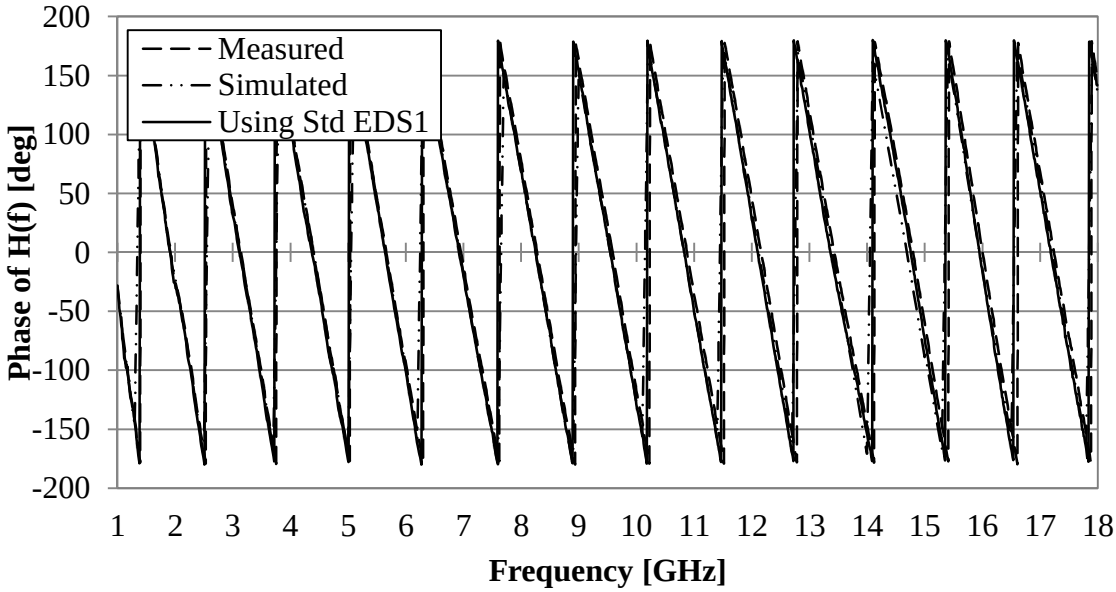

Figure 3.22. Comparison of the phase of CATF for SAAB2 obtained using three different approaches; two identical antenna measurement technique, two identical antenna simulations in FEKO, and two antenna measurement technique using CATF standard antenna EDS1.

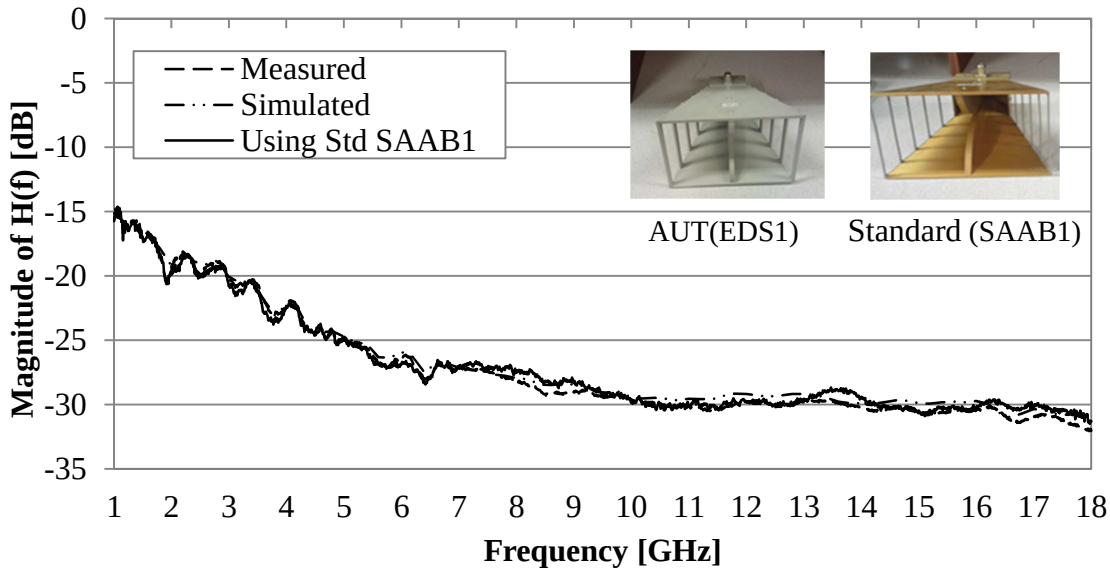

Figure 3.23. Comparison of the magnitude of CATF for EDS1 obtained using three different approaches; two identical antenna measurement technique, two identical antenna simulations in FEKO, and two antenna measurement technique using CATF standard antenna SAAB1.

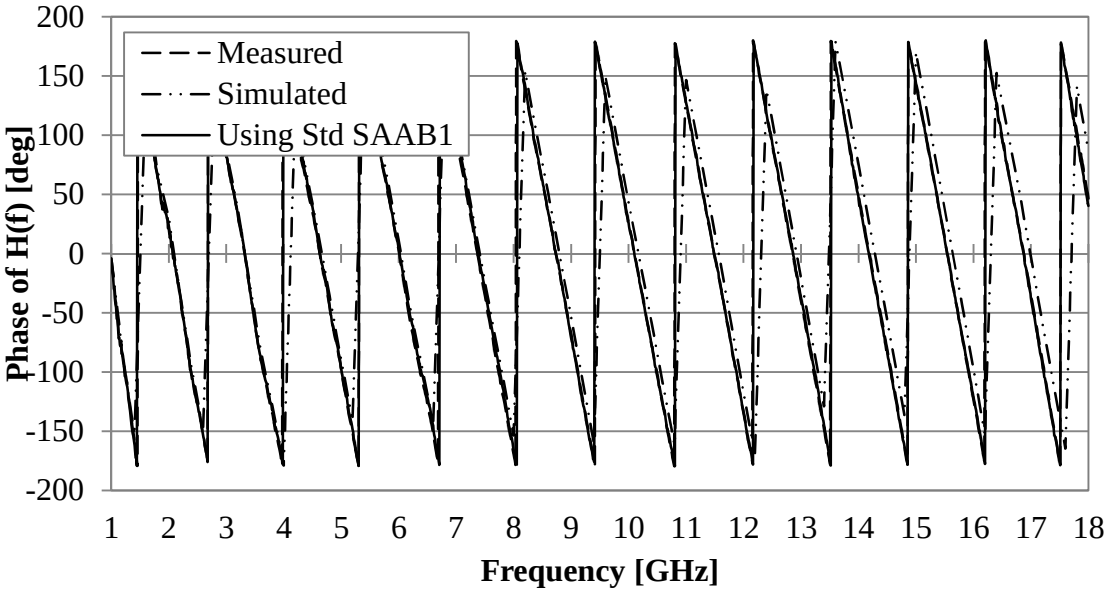

Figure 3.24. Comparison of the phase of CATF for EDS1 obtained using three different approaches; two identical antenna measurement technique, two identical antenna simulations in FEKO, and two antenna measurement technique using CATF standard antenna SAAB1.

In this section it was shown that anechoic chamber antenna measurements can be used to determine the CATF of an unknown antenna, if a reference antenna for which the CATF is known. The results were verified against data obtained using the identical two antenna measurement technique, and simulated data obtained using FEKO.

3.7. SUMMARY

At the beginning of this chapter a broad outline was given how the CATF of the DRGH antenna can be determined from measurements performed in an anechoic chamber. The CATF of a standard antenna was established by measuring the transmission between two identical antennas. FEKO simulations were performed, and used as verification to ensure that the CATF from measured results is correct. The measurement setup and techniques required for a well calibrated measurement were discussed in detail; these included the calibration of the VNA, connectors, adapters and cables that were required.

Time domain measurements were needed for each antenna pair to determine the time delay between the two antennas. The distance between the antennas was calculated from the measured time delay, as this was significantly more accurate than trying to use a measuring tape to measure the distance between the two antennas.

Transmission coefficients of the antennas were measured and distances between the antennas were calculated for each measurement setup. The CATF of each antenna was then compared to the simulated results in FEKO. The results compared very well. Measurements were also performed between a designated CATF standard antenna and another antenna that was not identical to the standard antenna. The determined CATF compared well to the simulated results of identical antennas and the measurements using two identical antennas in the anechoic chamber.

In Chapter 4 the CATF of an unknown antenna will be determined in the compact antenna test range, again using the CATF standard antenna characterised in Chapter 3.

CHAPTER 4 DETERMINATION OF THE CATF OF AN ANTENNA IN A CATR USING A STANDARD ANTENNA

4.1. INTRODUCTION

This chapter presents details on how the CATF standard antenna characterised in Chapter 3 can be used to determine the CATF of an unknown antenna in a compact antenna test range (CATR) facility. Even though the determination of the CATF of an unknown antenna is well established in an anechoic chamber and was described in some detail for a DRGH antenna in Chapter 3, the determination of the CATF of an unknown antenna by using a standard antenna in a CATR has not been described in the open literature before. The University of Pretoria has a CATR facility, and the establishment of the capability to calibrate UWB antennas in terms of their CATF will be a useful extension to the services which the facility can provide for research purposes and general industry support.

Measuring antenna radiation properties at microwave frequencies in an anechoic chamber may sometimes require a large chamber, depending on the size of the antenna and the frequency. A CATR is more versatile in terms of accommodating different antenna sizes over a wider frequency range, and the measurement setup is generally easier to do, e.g. the accurate determination of the distance between the transmit and receive antennas (for a setup in an anechoic chamber) is replaced by the requirement that the antenna standard and the antenna under test be placed at the same position in the CATR.

The characterisation of antennas in terms of their CATF in a CATR is discussed in Section 4.2. The equation used in the process is derived and measurement results are presented and verified. Section 4.3 discusses the uncertainty contributions for the magnitude and phase of the CATF for the measured antennas and Section 4.4 gives a short summary of the chapter.

4.2. CATF OF AN UNKNOWN ANTENNA USING A STANDARD ANTENNA IN A CATR

Since the CATF of different antennas were determined in the previous chapter, they can now be used as CATF standard antennas. The aim is now to use such a CATF standard antenna to determine the CATF of an unknown antenna under test (AUT), using the CATR facility. The most important issues to consider is the placement of the standard antenna and the AUT in the quiet zone of the CATR before measurements are done, and also the equation used to calculate the CATF from the two sets of measured data.

4.2.1. Standard antenna

Two antennas (EDS1 and SAAB1) were selected to be used as CATF standard antennas. Figure 4.1 to 4.4 shows the magnitudes and phases (as determined in Chapter 3) of the CATF of the two standard antennas used.

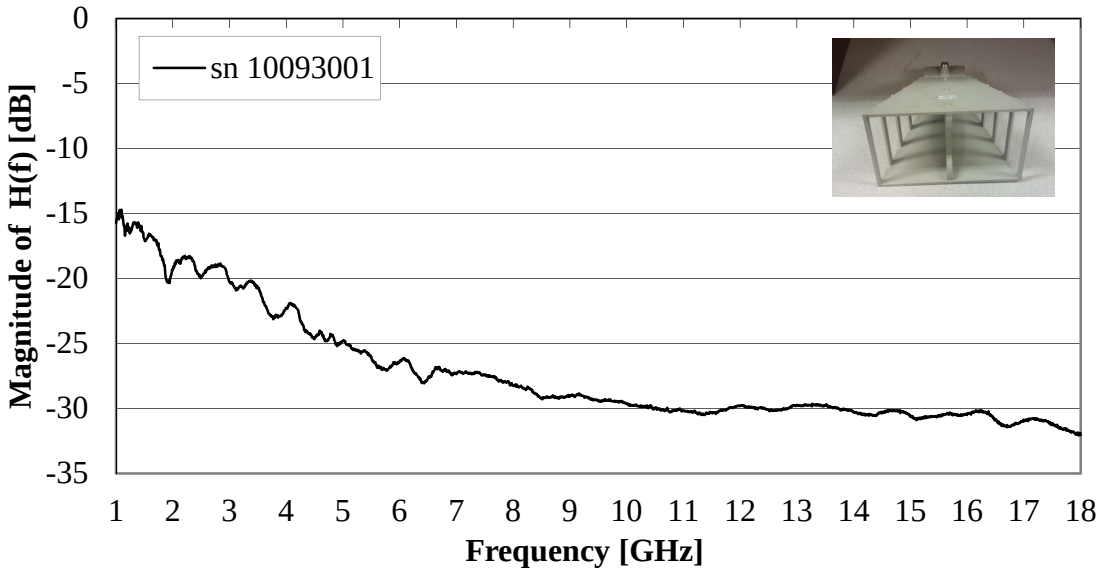

Figure 4.1. Magnitude of CATF of standard antenna EDS1.

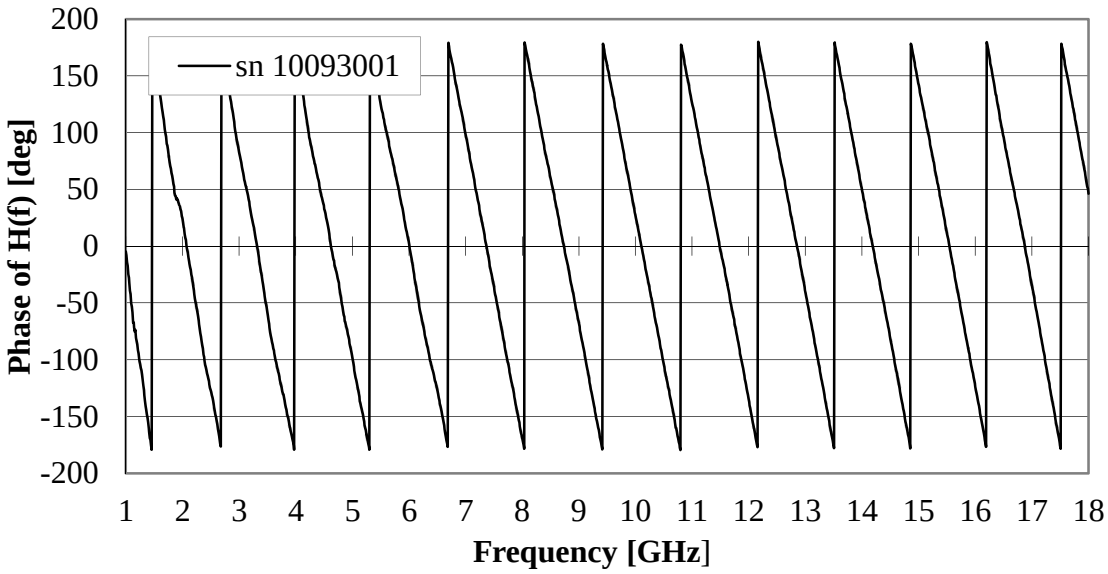

Figure 4.2. Phase of CATF of standard antenna EDS1.

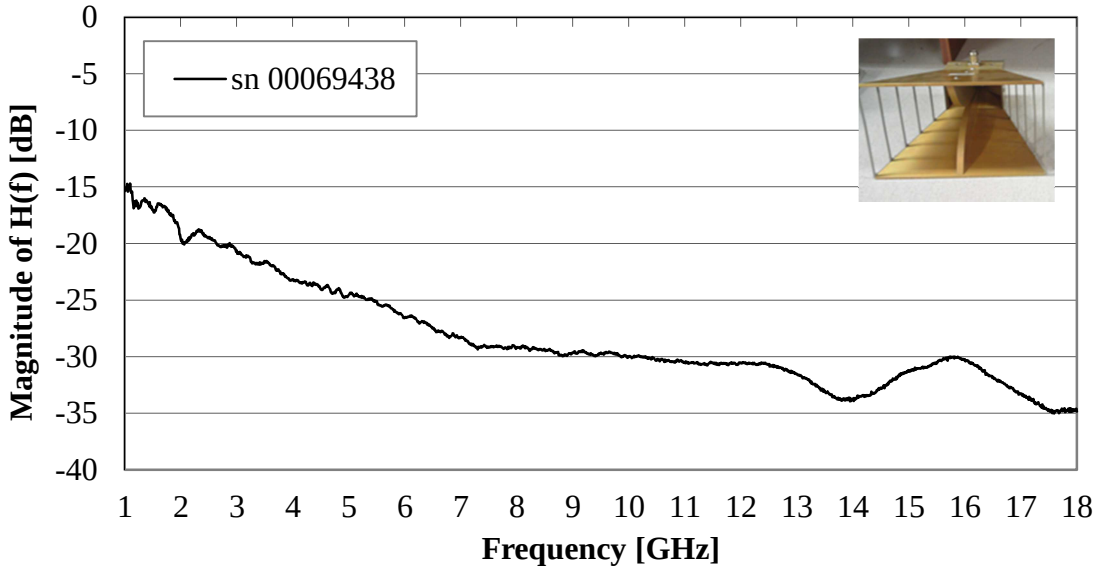

Figure 4.3. Magnitude of CATF of standard antenna SAAB1.

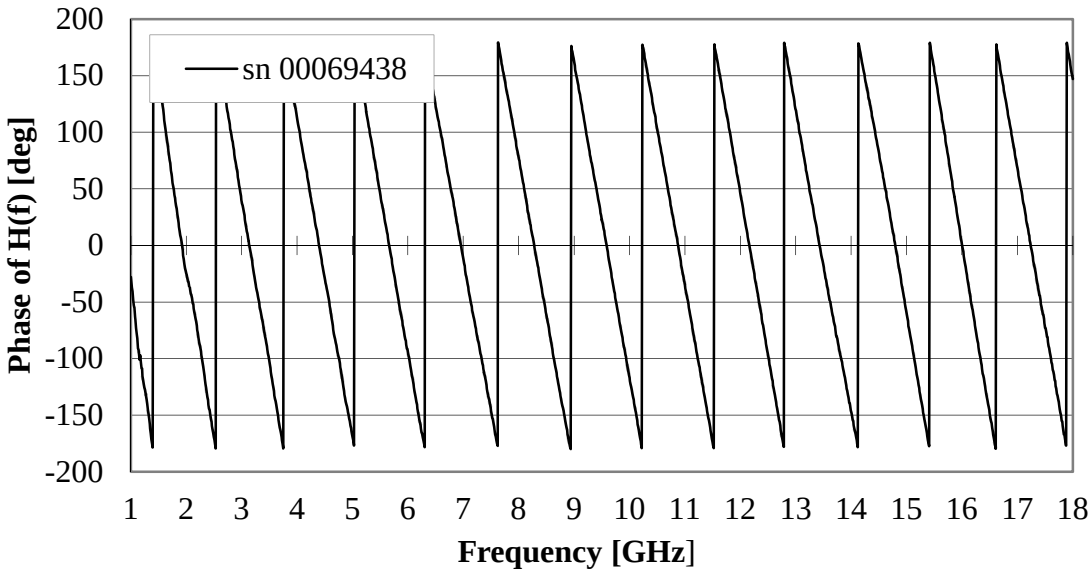

Figure 4.4. Phase of CATF of standard antenna SAAB1.

4.2.2. Measurement setup in the CATR

Figure 4.5 contains a schematic diagram of the measurement setup in the CATR. It is important to note that the standard antenna and the AUT may be different in size, and one must have a consistent and valid measurement procedure to ensure accurate determination of CATF in the CATR.

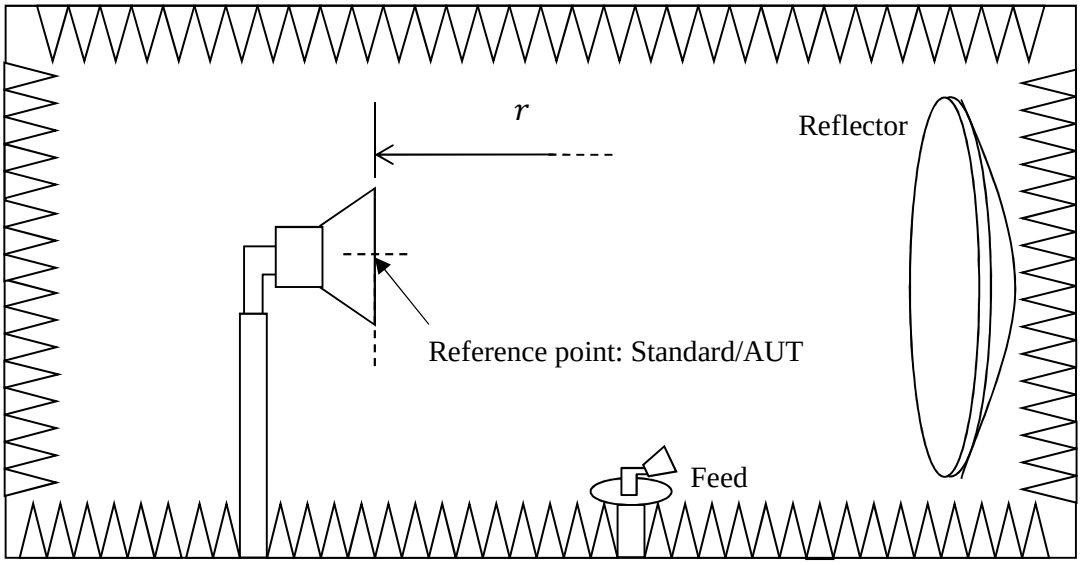

Figure 4.5. Schematic diagram of measurement setup in the CATR.

Figures 4.6 and 4.7 show photographs of the actual measurement setup in the CATR. Figure 4.6 shows the reference point to which all the antennas were aligned and Figure 4.7 shows a photograph of the complete measurement setup in the CATR.

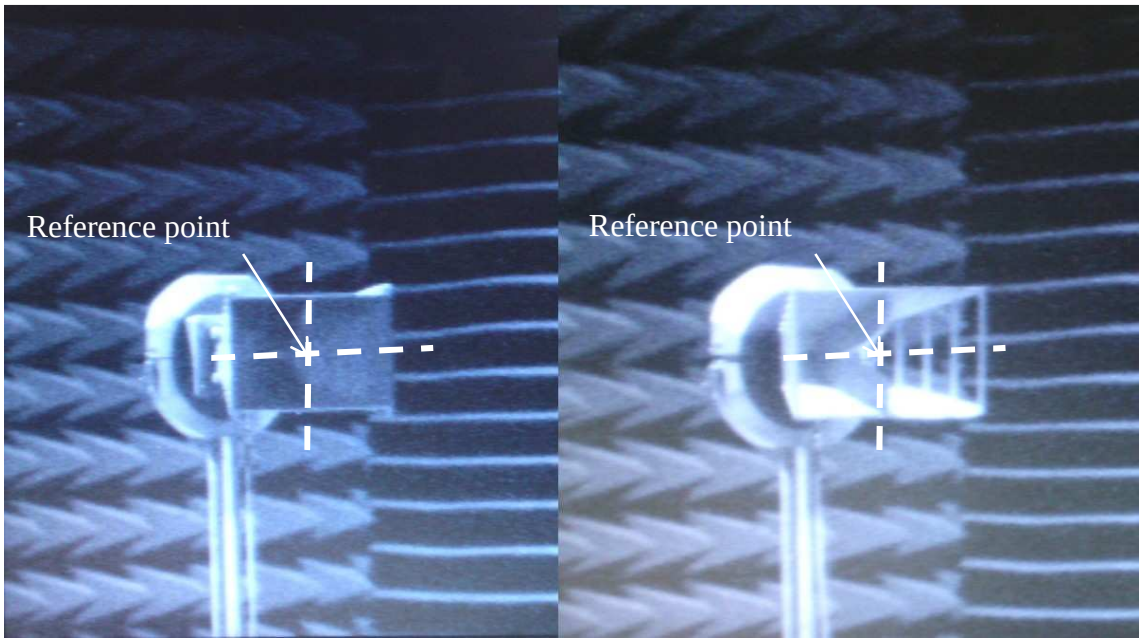

Figure 4.6. Photograph of standard antenna and AUT mounted in the CATR - the reference point is located in the middle of the aperture of the antenna.

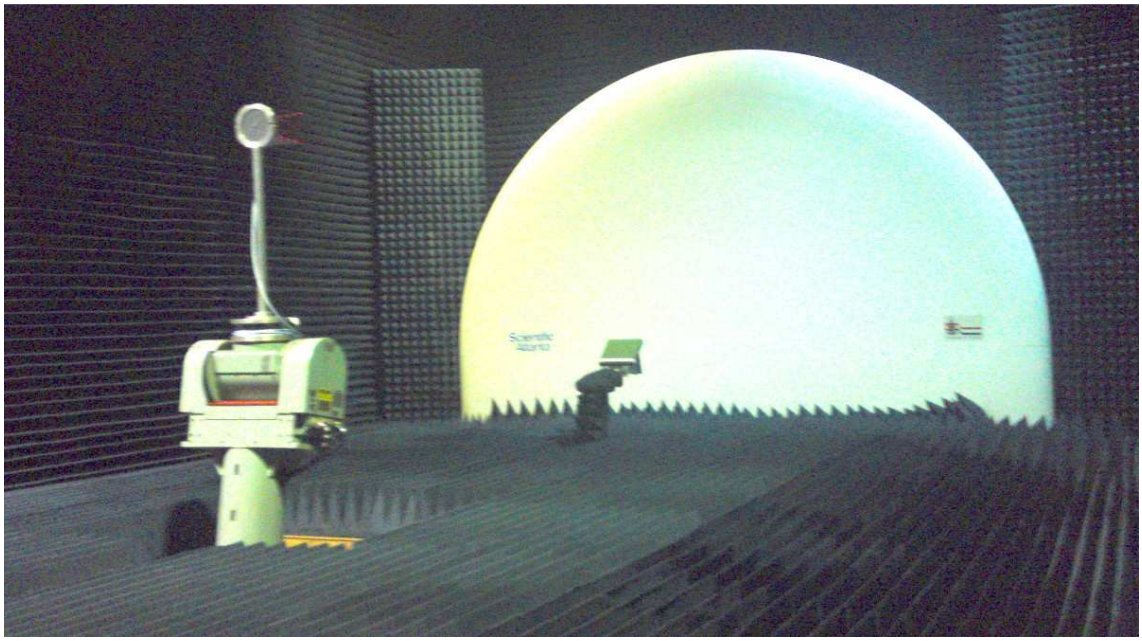

Figure 4.7. Photograph of measurement setup in the CATR.

4.2.3. Determination of the CATF in the CATR

The placement of the antennas in the CATR is an important part of the measurements setup to ensure that the measurements are performed correctly. An equation is derived in section 4.2.3.2 to determine the CATF of an UWB antenna with the measurements performed in the CATR.

4.2.3.1 Placement of antennas in the CATR

CATF is a complex quantity and to accurately determine the phase the distance between the antennas is very important when performing measurements which will be used to calculate the CATF. In the CATR the distance between the antennas (reflector and standard antenna, or reflector and AUT) was not determined using the same time domain measurement technique as for the anechoic chamber measurements. The technique used in the CATR was by identifying a reference point in the quite zone of the CATR. Both the standard antenna and the AUT were then positioned, using a theodolite, (consecutively, because two measurements needs to be performed) in the CATR such that the reference point was located in the centre of the radiating apertures of the antennas. The apertures of the antennas were thus positioned in the same reference plane, and on the same centre line, so that they will both be exactly the same distance away from the reflector.

Figure 4.8 shows how the antennas were placed in the CATR with reference to the reflector for the two measurements. r is the distance in the compact antenna test range from the reflector to the reference point where the radiating apertures were aligned. The absolute value of r was not measured, and is not important, because both antennas were placed exactly the same distance away from the reflector.

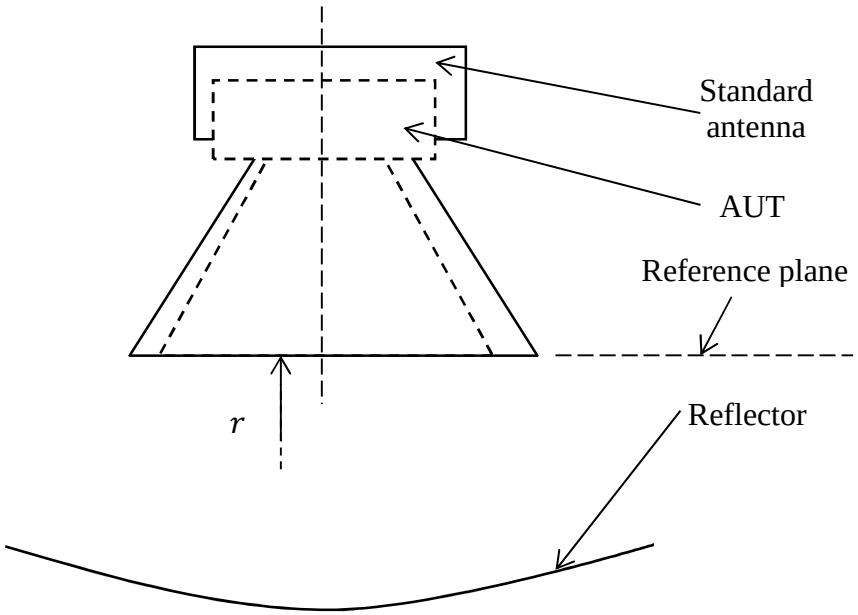

Figure 4.8. Schematic diagram to show the position of the reference plane for the antennas mounted in the CATR.

4.2.3.2 Equation for determination of the CATF from measurements in the CATR

An equation to determine the CATF using the measurements performed in the CATR needs to be derived. Two measurements are required to determine the CATF of an AUT. The first setup and measurement is with the standard antenna, and the second with the unknown AUT. Equation (4.1) is an expression for the CATF of the CATR (feed with parabolic dish), with r_1 an unknown distance in the CATR, $\bar{H}_{Std}$ the known CATF of the standard antenna, $\bar{K}(\omega, r_1)$ a complex transfer coefficient specific to the CATR, and S_{21_Std} the transmission coefficient that was measured in the CATR.

$$\bar{H}_{CATR\_1} = \frac{1}{\bar{H}_{Std}} \bar{K}(\omega, r_1) \bar{S}_{21\_Std} e^{\frac{j\omega r_1}{c}} \tag{4.1}$$

Equation (4.2) is an expression for the CATF of the feed inside the CATR as obtained from the second measurement when the standard antenna was substituted with the unknown AUT. $\bar{H}_{AUT}$ is the unknown CATF of the AUT, r_2 (in general) is the unknown

distance in the CATR, $\bar{K}(\omega, r_2)$ a complex transfer coefficient specific to the CATR, and S_{21_AUT} is the measured transmission coefficient in the CATR.

$$\bar{H}_{CATR\_2} = \frac{1}{\bar{H}_{AUT}} \bar{K}(\omega, r_2) \bar{S}_{21\_AUT} e^{\frac{j\omega r_2}{c}} \tag{4.2}$$

Knowing that the CATF of the CATR did not change we can assume that $\bar{H}_{CATR\_1} = \bar{H}_{CATR\_2}$ if we ensure that $r_1 = r_2 = r$ (by placing the antennas with the centres of their apertures at the same reference point). The CATF of the AUT can then be determined by equation (4.4), or with equation (4.6) after further simplification.

$$\frac{1}{\bar{H}_{Std}} \bar{K}(\omega, r_1) \bar{S}_{21\_Std} e^{\frac{j\omega r_1}{c}} = \frac{1}{\bar{H}_{AUT}} \bar{K}(\omega, r_2) \bar{S}_{21\_AUT} e^{\frac{j\omega r_2}{c}} \tag{4.3}$$

$$\bar{H}_{AUT} = \bar{H}_{Std} \frac{\bar{K}(\omega, r_2)}{\bar{K}(\omega, r_1)} \frac{\bar{S}_{21\_AUT}}{\bar{S}_{21\_Std}} e^{\left(\frac{j\omega r_2}{c}\right) + \left(\frac{-j\omega r_1}{c}\right)} \tag{4.4}$$

$$\bar{H}_{AUT} = \bar{H}_{Std} \frac{\bar{S}_{21\_AUT}}{\bar{S}_{21\_Std}} e^{\frac{j\omega}{c}(r_2 - r_1)} \tag{4.5}$$

$$\bar{H}_{AUT} = \bar{H}_{Std} \frac{\bar{S}_{21\_AUT}}{\bar{S}_{21\_Std}} \tag{4.6}$$

4.2.4. CATF results as determined from measurements in the CATR

Two antenna sets were measured in the CATR to determine the CATF of two different antennas under test (SAAB2 and EDS1). The results were compared to previously obtained results from Chapter 3.

Figures 4.9 and 4.10 show the CATF of antenna SAAB2 as determined from measurements in the CATR, using antenna EDS1 as the standard antenna. These new results are compared to simulated results for SAAB2 using FEKO, as well as the results obtained in the anechoic chamber using two identical antennas. The results compare well.

In Figures 4.11 and 4.12 the CATF of antenna EDS1 are shown, where the standard antenna SAAB1 was used in the CATR. The identical antennas were measured in the anechoic chamber with antenna EDS1 and EDS2. The simulated results were performed in FEKO, with the model for the antenna EDS1. Good comparison is observed between the three sets of data.

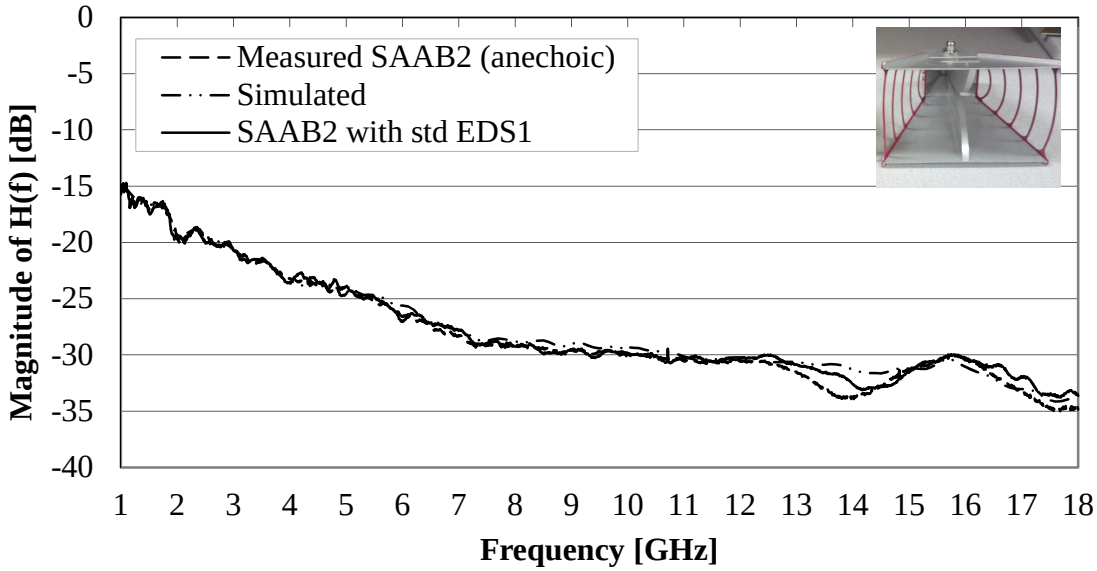

Figure 4.9. Magnitude of $\overline{H}(f)$ of SAAB2, using EDS1 as the standard antenna.

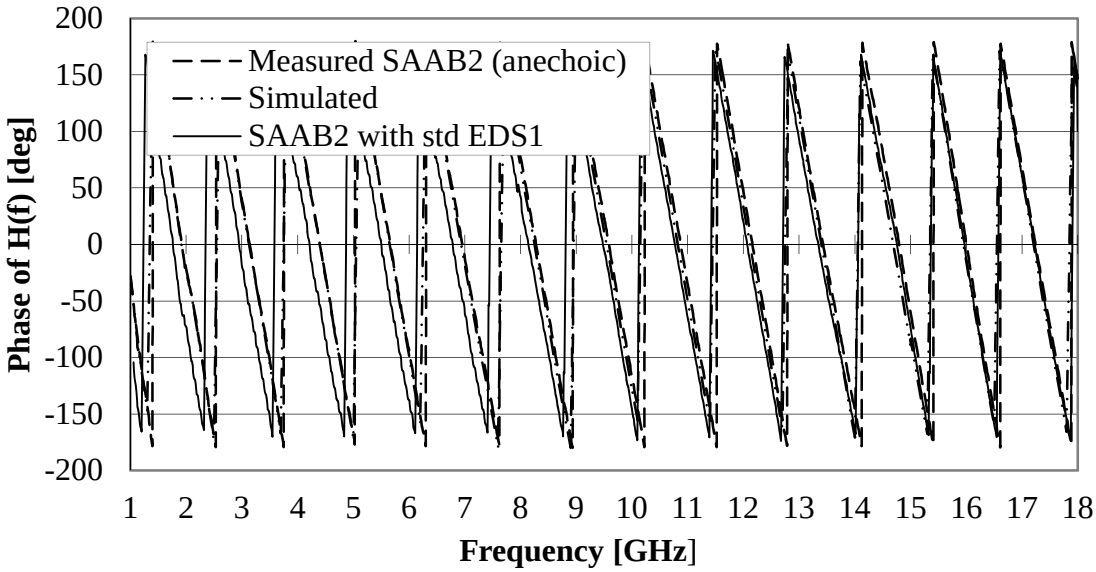

Figure 4.10. Phase of $\overline{H}(f)$ of SAAB2, using EDS1 as the standard antenna.

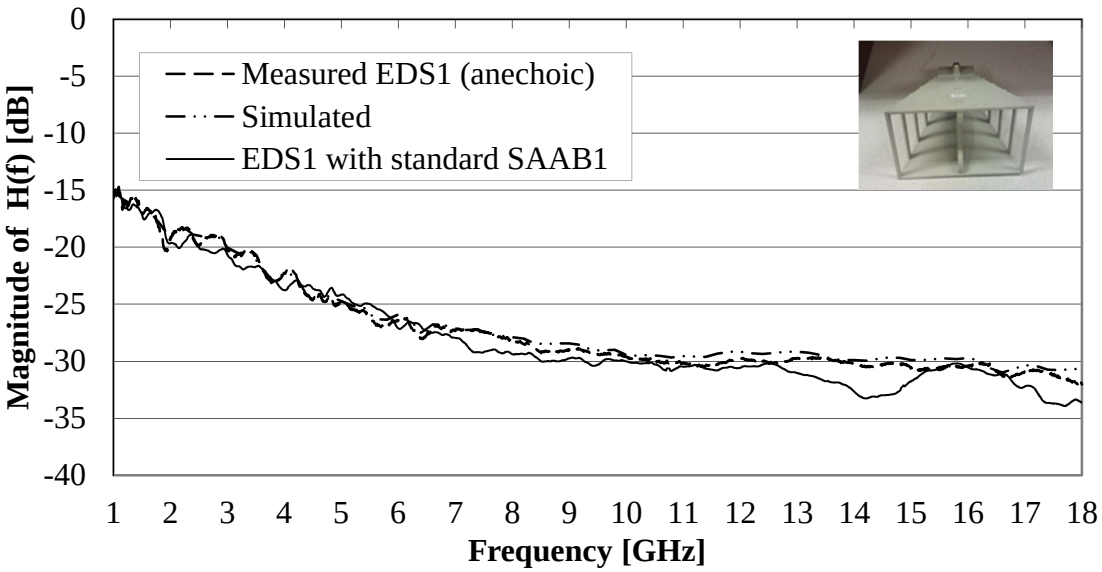

Figure 4.11. Magnitude of $\bar{H}(f)$ of EDS1, using SAAB1 as the standard antenna.

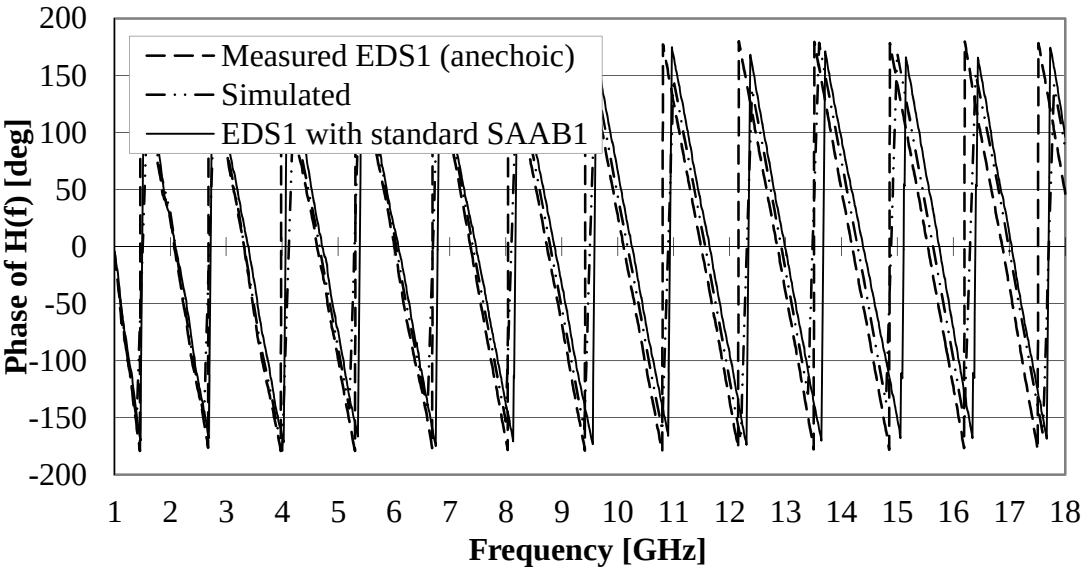

Figure 4.12. Phase of $\bar{H}(f)$ of EDS1, using SAAB1 as the standard antenna.

All the antennas measured compared very well with the simulated results in FEKO and the two identical antenna measurements in the anechoic chamber. The minor differences between the different sets of CATF can be due to a number of factors, e.g., antennas not being 100% identical, placement of the antennas in the CATR etc. In the next section errors and uncertainties of these measurements are analysed.

4.3. UNCERTAINTY CONTRIBUTIONS

To evaluate the results quantatively, the error contributions of the measured data needs to be analysed. Typical errors and uncertainties of measurements performed in the CATR to determine the CATF are; the contribution from the standard, connection repeatability, waveguide port reflection, range reflections, resolution, cable leakage, cable flexing, mechanical error, fixed phase errors from port to port and cable phase variations due to temperature. These will be discussed in some detail in the paragraphs below, with uncertainty budgets for the different frequency ranges presented in Addendum A.

The uncertainty contribution from the standard antenna comes from the measurements performed in the anechoic chamber. These CATF results were used as an input to the measurements performed in the CATR. The uncertainties in the anechoic chamber will not be discussed in detail, but typical contributions are: how accurate the distance can be determined between the antennas, 'identical' antennas, reflection, mismatch, leakage etc. The final uncertainties from the measurements in the anechoic chamber were typically between 0.5 and 1 dB and 5 and 12 degrees for well-matched antennas. Needs evidence

Connection repeatability is defined by the changes that occur every time a new connection is made. A connection between the AUT and the cable and also the standard antenna, the contribution for the connector repeatability was experimentally measured by taking the worst case ESDM (estimated standard deviation of the mean) of the measurements. Uncertainty contributions of 0.085 dB and 0.66 degrees were obtained for connector repeatability.

The contribution due to the reflection loss at the waveguide port was determined by taking the reflections at the port into account, these were experimentally obtained for the UUT and the VSWR of the standard antenna was 1.065 as in [30]. An uncertainty contribution of 0.1 dB and 0.6 deg were obtained. Equation (4.7) gives the maximum mismatch error limits in dB for the magnitude and equation (4.8) the maximum phase error. ρ_1 and ρ_2 are the voltage reflection coefficients (VRC) of the UUT and the mating waveguide, respectively.

$$20log10(1 \pm |\rho_1 \rho_2|) \text{ [dB]} \tag{4.7}$$

$$\pm sin^{-1}|\rho_1 \rho_2| \text{ [deg]} \tag{4.8}$$

The range reflection, R, was taken as -70 dB, the measured signal -40 dB and the absorber reflection is typically -50 dB, which is deemed conservative [30]. Equation (4.9) shows how to calculate the contribution for the budget in dB.

$$U_{refl} = 20\log(1) \pm 10^{\frac{R}{20}} \tag{4.9}$$

When R is equal to -70 dB a value of 0.0003 dB was obtained for U_{refl}, which is included in the uncertainty budget.

The resolution of the magnitude and phase are determined by taking the worst case of half of the amplitude per measurement step, respectively. This was experimentally determined by looking at the measured data and an uncertainty contribution of 0.05 dB and 2.75 degrees were obtained.

The cables were specified for >90 dB for the minimum screening effectiveness, this contribution was deemed negligible. As well as cable flexing, cables were moved minimally, so this contribution was also negligible. Although it does have a larger effect on the phase measurements, these were already taken into account when the connector repeatability was measured.

The mechanical setup, alignment of the antennas, levelling etc., have little effect on the magnitude of the CATF. This effect was assumed to be negligible. On the other hand, the alignment of the antennas is probably the largest contributor to uncertainty in the phase of the CATF. Because it is difficult to place the antennas on the exact same reference point in the CATR, a theodolite was used to assist with the accurate placement of the antennas in the CATR to the best of our ability. By performing a number of numerical calculations the

phase error was determined for slight variations in the placement of the antenna and found to be between 5 and 20 degrees for a placement error of 2 mm.

Fixed phase errors from port to port were corrected for in the measurements, so no need to apply an uncertainty contribution to it.

Cable phase variations due to temperature are also negligible. The measurements were performed in a controlled environment where very little temperature variation occurred during the time span of the measurement.

The expanded uncertainties of measurement, for measuring an AUT in a CATR using a standard reference antenna, were calculated with a coverage factor of $k = 2$ which approximates to a confidence level of 95.45%. The complete uncertainty budgets can be found in Addendum A. Figures 4.13 and 4.14 show the uncertainty of measurement on the magnitude and the phase of the CATF of antenna EDS1 as measured in the CATR using antenna SAAB1 as standard antenna. The estimated measurement uncertainty in the magnitude of the CATF varies between 1.25 and 2.7 dB, and the phase uncertainty varies between 14.9 and 33.7 degrees. For the example shown in Figures 4.13 and 4.14 the two sets of additional (FEKO data and two antenna method measured data) data are within the measurement uncertainty range for almost the entire frequency range.

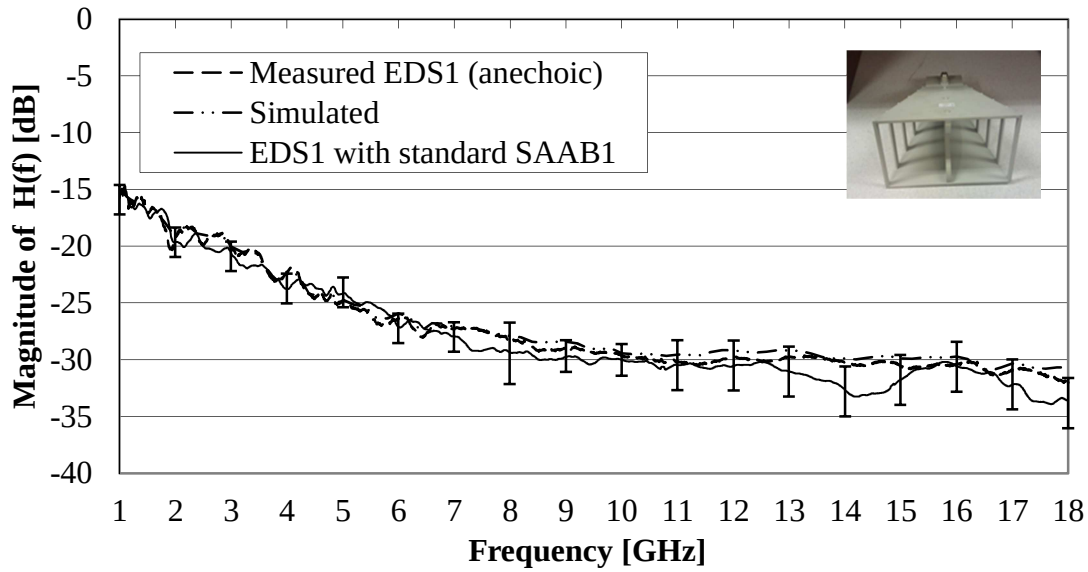

Figure 4.13. The magnitude of $\bar{H}(f)$ for antenna EDS1 with error bars, indicating the uncertainty of measurement.

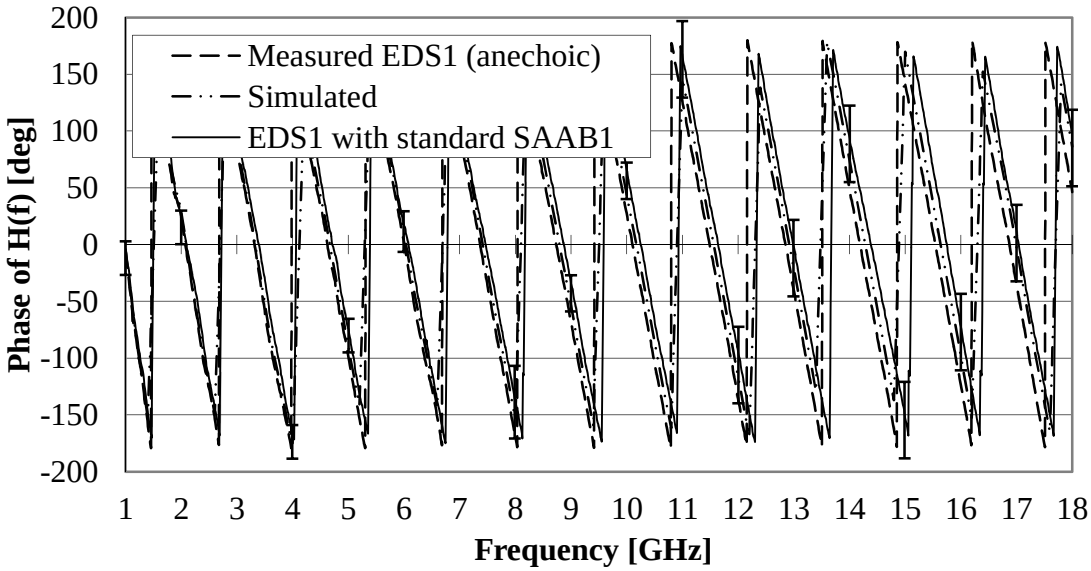

Figure 4.14. The phase of $\bar{H}(f)$ of antenna EDS1 with error bars, indicating the uncertainty of measurement.

4.4. SUMMARY

In this chapter it was shown that the CATF of a DRGH antenna can be measured in the CATR using a standard antenna and a modified gain-transfer technique. The CATF of the standard antennas were determined in Chapter 3. The modifications to the well-known

gain-transfer method involved the use of a fixed reference point in the CATR to mount the standard and the unknown antennas, and the use of complex measured transmission data to accurately determine the magnitude and phase of the CATF.

The measurement setup in the CATR was described in detail – and the importance of correct placement in the CATR highlighted because of the importance it plays, especially in the phase results of the CATF.

The CATF results of the unknown antennas were compared to simulated results and results obtained from the measurements in an anechoic chamber. The results compared well within the uncertainty limits. Uncertainty contributions for these measurements were evaluated and displayed to give an indication of the errors expected.

CHAPTER 5 CONCLUSION

The main objective of this dissertation was to establish a CATF measurement technique using the CATR at the University of Pretoria. A standard antenna first had to be characterised, and then the gain-transfer method in the CATR had to be adapted to accommodate the measurement of complex transmission coefficient and determination of CATF. The frequency range of 1 – 18 GHz was focused on.

The literature study conducted in Chapter 2 revealed a number of studies that have been done with two identical antennas in an anechoic chamber. No study could be found on the measurement of CATF in the CATR.

Two identical antennas were measured in the anechoic chamber to get familiar with the measurement procedure as used in literature. In Chapter 3 a number of DRGH antennas were measured to determine the CATF of a standard antenna. Measurements were done successfully and compared to a numerical model of the antenna simulated in FEKO.

Various antennas were measured in the CATR using the standard antennas to determine the CATF of an unknown AUT. These were presented in Chapter 4. Uncertainty contributions were discussed and used to pinpoint where the measurements method can be improved.

In conclusion, the hypothesis that the CATF of an antenna can be determined in the CATR was proven. A good comparison was found between simulated results, the CATF results obtained in the anechoic chamber, and the results obtained in the CATR. This validates the procedure and equation of obtaining the CATF of an UWB antenna in the CATR using a known standard antenna.

5.1. CONTRIBUTION TO THE MEASUREMENT OF THE CATF OF UWB ANTENNAS

A short summary of the contributions made by this study is given below:

- The CATF of a standard antenna was determined – in this case a UWB DRGH antenna.
- A modified gain-transfer method was developed to determine the CATF of unknown wideband antennas in a CATR.
- The equation for determining the CATF of an unknown antenna in the CATR was derived and validated.
- Uncertainty contributions associated with the measurements were investigated.

5.2. FUTURE WORK

While conducting this study the following possible future research with regard to CATF were identified:

Accurate measurements of the distance: There is a need to measure the distance r between the two antennas in the anechoic chamber more accurately, as it has a large effect on the phase results of the standard antenna. This will lead to more accurate measurements in the CATR and reduce the uncertainty of measurement.

Phase correction between different feed antennas in the CATR: In the CATR, two feed antennas were required to measure the complete frequency range from 1 to 18 GHz. It was noticed that there was a phase shift when changing from the one feed antenna to another. A correction was made for this in the results for this dissertation, but introduced larger uncertainty in the phase results, especially at the higher frequencies. Studies on how this phase shift can be better corrected for or eliminated are recommended.

Different kinds of antennas to be measured against the standard antenna: In this dissertation very similar antennas were measured against one another. Further studies on

measuring different types of antennas with similar frequency ranges are recommended, as ideally one only wants to have a few standard antennas and not one for each and every type of antenna, as this has a cost implication in manufacturing identical antennas of each type.

REFERENCES

[1] W. Sörgel and W. Wiesbeck, "Influence of the antennas on the ultra wideband transmission," *EURASIP Journal on Applied Signal Processing*, no. 3, pp. 296-305, 2005.

[2] A. Bayram, A. M. Attiya and A Safaai-Jasi, "Frequency-Domain measurement of indoor UWB channels," *Microwave and Optical Technology letters*, vol. 44, no. 2, pp. 118-123, 20 Jan. 2005.

[3] S. Yiqiong, S. Aditya and C. L. Law, "Transfer function characterization of UWB antennas based on frequency domain measurement," *European Microwave Conference*, vol. 3, pp. 4-pp, 4-6 Oct. 2005.

[4] X. Qing and Z. N. Chen, "Transfer function measurement for UWB antenna," *IEEE Antennas and Propagation Society Symposium*, vol. 3, pp. 2532-2535, Jun. 2004.

[5] A. H. Mohammadian, A. Rajkotia and S. S. Soliman, "Characterization of UWB transmit and receive antenna system," *IEEE Conference on Ultra Wideband Systems and Technologies*, pp. 157-161, Nov. 2003.

[6] H. Hosoyama, T. Iwasaki and S. Ishigami, "Evaluation of the complex antenna factor of a dipole antenna by measuring the S-parameters of the balun," *Electrical Engineering in Japan*, vol. 123, no. 2, pp. 16-23, 1998.

[7] X. Qing, Z. N. Chen and M. Y. W. Chai, "Network approach to UWB antenna transfer functions characterization," *European Microwave Conference*, vol. 3, pp. 4-pp, 4-6 Oct. 2005.

[8] Y. Duroc, A. Ghiotto, T. P. Vuong and S. Tedjini, "UWB antennas: System with transfer function and impulse response," *IEEE Transactions on Antennas and Propagation*, vol. 55, no. 5, pp. 1449-1451, May 2007.

[9] Y. Duroc, R. Khouri, V. Beroulle, T. P. Vuong and S. Tedjini, "Considerations on the characterization and the modelization of ultra-wideband antennas," *IEEE International Conference on Ultra Wideband, ICUWB*, pp. 491-496, Sept. 2007.

[10] Y. Duroc, T. P. Vuong and S. Tedjini, "A time/frequency model of ultra wideband antennas," *IEEE Transactions on Antennas and Propagation*, vol. 55, no. 8, pp. 2342-2350, Aug. 2007.

[11] Y. Duroc, A. Ghiotto, T. P. Vuong and S. Tedjini, "On the characterization of UWB antennas," *International Journal of RF and Microwave Computer-aided Engineering*, vol. 19, Issue 2, pp. 258-269, Mar. 2009.

[12] W. Wiesbeck, G. Adamiuk and C. Sturm, "Basic properties and design principles of UWB antennas," *Proceedings of the IEEE*, vol. 97, no. 2, pp. 372-385, Feb. 2009.

[13] S. Licul and W. A. Davis, "Ultra-wideband (UWB) antenna measurements using vector network analyzer," *IEEE Antennas and Propagation Society Symposium*, vol. 2, pp. 1319-1322, June 2004.

[14] T. Iwasaki and K. Tomizawa, "Systematic uncertainties of complex antenna factor of a dipole antenna as determined by two methods," *IEEE Transactions on Electromagnetic Compatibility*, vol. 46, no. 2, pp. 234-245, 2004.

[15] T. Iwasaki and K. Tomizawa, "Measurement of S-parameters of balun and its application to determination of complex antenna factor," *IEEE International Symposium on Electromagnetic Compatibility*, vol. 1, pp. 62-65, May 2003.

[16] H. Hosoyama, T. Iwasaki and S. Ishigami, "Complex antenna factor of a V-dipole antenna with two coaxial feeders for field measurements," *IEEE Transactions on Electromagnetic Compatibility*, vol. 41, no. 2, pp. 154-158, May 1999.

[17] S. Ishigami, H. Iida and T. Iwasaki, "Measurements of complex antenna factor by the near-field 3-antenna method," *IEEE Transactions on Electromagnetic Compatibility*, vol. 38, no. 3, pp. 424-432, 1996.

[18] K. Fujii, S. Ishigami and T. Iwasaki, "Evaluation of complex antenna factor of dipole antenna by near-field 3-antenna method and method of moment," *Electronics and Communications in Japan*, Part 1, vol. 80, no. 11, pp. 34-44, 1997.

[19] J. McLean, R. Sutton and R. Hoffman, "Interpreting antenna performance parameters for EMC applications: Part 3: Antenna factor," *TKDRF solutions Inc.*, pp. 18-26, 2004.

[20] H. Foltz, J. S. McLean, A. Medina, J. Li and R. Sutton, "UWB antenna transfer functions using minimum phase functions," *IEEE International Symposium on Antennas and Propagation*, pp. 1413-1416, Jun. 2007.

[21] J. S. McLean, R. Sutton, A. Medina, H. Foltz and J. Li, "The experimental characterization of UWB antennas via frequency domain measurements," *IEEE Antennas and Propagation Magazine*, vol. 49, no. 6, pp. 192-202, Dec. 2007.

[22] J. S. McLean and R. Sutton, "UWB antenna characterization," *Proceedings of the IEEE International Conference on Ultra-wideband*, vol. 2, pp. 113-116, Sept. 2008.

[23] B. Jacobs, "The effect of manufacturing and assembling tolerances on the performance of 1-18 GHz double ridged guide horn," Masters dissertation, University of Pretoria, 2010.

[24] EM Software & Systems, FEKO User's Manual, Suite 5.4, July 2008.

[25] W. L. Stutzman and G. A. Thiele, Antenna Theory and Design, Wiley, 1998

[26] IEEE Standard Test Procedures for Antennas, IEEE Standard 149, 1979.

[27] C. A. Balanis, Antenna theory: Analysis and design, Wiley, 1997.

[28] Octave, John W. Eaton , GNU Octave.

[29] MatLab, TheMathWorks Inc., 2010.

[30] Laboratory procedure: P-745-06, Internal report, Business Enterprises at the University of Pretoria, Dec 2009.

ADDENDUM A: UNCERTAINTY BUDGETS

The uncertainty budgets, including the error contributions, for different frequency ranges for magnitude and phase of the CATF are shown in this section. The final uncertainty of measurements gives an idea of how good the measurements compare to one another.

The uncertainty budgets are shown for measurements performed in the CATR using a standard antenna to determine the CATF for an AUT. Table A1 to A5 show the uncertainties for the magnitude of CATF and Table A6 to A10 the phase uncertainties. Typical contributions are the estimated uncertainty for the standard, connection repeatability, waveguide port reflection, range reflections, resolution, cable leakage, cable flexing, mechanical error, fixed phase errors from port to port and cable phase variations due to temperature. The expanded uncertainties of measurement were calculated with a coverage factor of $k = 2$ which approximates to a confidence level of 95.45%.

Table A1. Magnitude Uncertainty, frequency range 1 GHz – 5 GHz.

Symbol	Source of uncertainty	Estimated uncertainty	Unit	Probability distribution	Sensitivity coefficient	Standard uncertainty contribution	Reliability	Remarks
Std	Measured from anechoic chamber	0.5	dB	1	1	0.5	100	Max difference between FEKO and two antenna method were used
Range _Refl	Compact range reflection	0.0003	dB	$\sqrt{3}$	1	0.00018	100	$20log1 \pm 10^{\frac{R}{20}}$ $R = -70$
Mis	Mismatch	0.1	dB	$\sqrt{2}$	1	0.07071	100	$20log10(1 \pm \rho_1\rho_2)$
Cable	Cable screening and reflection	0	dB	$\sqrt{3}$	1	0	100	Negligible
RtoR	Range to range measurements, change in antenna	0.0061	dB	$\sqrt{3}$	1	0.0035	100	Difference in measured values from one range to another range
Refl loss	Reflection from port to connection	0.5	dB	$\sqrt{2}$	1	0.356	100	
Mech	Measurement setup, level, same reference point	0	dB	$\sqrt{3}$	1	0	100	Negligible
Res	AUT resolution	0.05	dB	$\sqrt{3}$	1	0.0288	100	Max dB change in one frequency step
Data	ESDM of data	0.085	dB	1	1	0.085	100	ESDM of data
Uncertainty of measurement k = 2			95.45%			1.25	dB	

Table A2. Magnitude Uncertainty, frequency range 5 GHz – 7GHz.

Symbol	Source of uncertainty	Estimated uncertainty	Unit	Probability distribution	Sensitivity coefficient	Standard uncertainty contribution	Reliability	Remarks
Std	Measured from anechoic chamber	0.5	dB	1	1	0.5	100	Max difference between FEKO and two antenna method were used
Range_ Refl	Compact range reflection	0.0003	dB	$\sqrt{3}$	1	0.00018	100	$20log1 \pm 10^{\frac{R}{20}}$ $R = -70$
Mis	Mismatch	0.1	dB	$\sqrt{2}$	1	0.07071	100	$20log10(1 \pm \rho_1\rho_2)$
Cable	Cable screening and reflection	0	dB	$\sqrt{3}$	1	0	100	Negligible
RtoR	Range to range measurements, change in antenna	0.01	dB	$\sqrt{3}$	1	0.0058	100	Difference in measured values from one range to another range
Refl loss	Reflection from port to connection	0.5	dB	$\sqrt{2}$	1	0.356	100	
Mech	Measurement setup, level, same reference point	0	dB	$\sqrt{3}$	1	0	100	Negligible
Res	AUT resolution	0.05	dB	$\sqrt{3}$	1	0.0288	100	Max dB change in one frequency step
Data	ESDM of data	0.085	dB	1	1	0.085	100	ESDM of data
Uncertainty of measurement k = 2 95.45%						1.25	dB	

Table A3. Magnitude Uncertainty, frequency range 7 GHz – 8 GHz.

Symbol	Source of uncertainty	Estimated uncertainty	Unit	Probability distribution	Sensitivity coefficient	Standard uncertainty contribution	Reliability	Remarks
Std	Measured from anechoic chamber	0.5	dB	1	1	0.5	100	Max difference between FEKO and two antenna method were used
Range_ Refl	Compact range reflection	0.0003	dB	$\sqrt{3}$	1	0.00018	100	$20log1 \pm 10^{\frac{R}{20}}$ $R = -70$
Cable	Cable screening and reflection	0	dB	$\sqrt{3}$	1	0	100	Negligible
Mis	Mismatch	0.1	dB	$\sqrt{2}$	1	0.07071	100	$20log10(1 \pm \rho_1\rho_2)$
RtoR	Range to range measurements, change in antenna	2	dB	$\sqrt{3}$	1	1.155	100	Difference in measured values from one range to another range
Refl loss	Reflection from port to connection	0.5	dB	$\sqrt{2}$	1	0.356	100	
Mech	Measurement setup, level, same reference point	0	dB	$\sqrt{3}$	1	0	100	Negligible
Res	AUT resolution	0.05	dB	$\sqrt{3}$	1	0.0288	100	Max dB change in one frequency step
Data	ESDM of data	0.085	dB	1	1	0.085	100	ESDM of data
Uncertainty of measurement k = 2			95.45%			2.7	dB	

Table A4. Magnitude Uncertainty, frequency range 8 GHz – 10 GHz.

Symbol	Source of uncertainty	Estimated uncertainty	Unit	Probability distribution	Sensitivity coefficient	Standard uncertainty contribution	Reliability	Remarks
Std	Measured from anechoic chamber	0.5	dB	1	1	0.5	100	Max difference between FEKO and two antenna method were used
Range_ Refl	Compact range reflection	0.0003	dB	$\sqrt{3}$	1	0.00018	100	$20log1 \pm 10^{\frac{R}{20}}$ $R = -70$
Mis	Mismatch	0.1	dB	$\sqrt{2}$	1	0.07071	100	$20log10(1 \pm \rho_1\rho_2)$
Cable	Cable screening and reflection	0	dB	$\sqrt{3}$	1	0	100	Negligible
RtoR	Range to range measurements, change in antenna	0.0017	dB	$\sqrt{3}$	1	0.00098	100	Difference in measured values from one range to another range
Refl loss	Reflection from port to connection	0.5	dB	$\sqrt{2}$	1	0.356	100	
Mech	Measurement setup, level, same reference point	0	dB	$\sqrt{3}$	1	0	100	Negligible
Res	AUT resolution	0.05	dB	$\sqrt{3}$	1	0.0288	100	Max dB change in one frequency step
Data	ESDM of data	0.085	dB	1	1	0.085	100	ESDM of data
Uncertainty of measurement k = 2 95.45%						1.3	dB	

Table A5. Magnitude Uncertainty, frequency range 10 GHz – 18 GHz.

Symbol	Source of uncertainty	Estimated uncertainty	Unit	Probability distribution	Sensitivity coefficient	Standard uncertainty contribution	Reliability	Remarks
Std	Measured from anechoic chamber	1	dB	1	1	1	100	Max difference between FEKO and two antenna method were used
Range_ Refl	Compact range reflection	0.0003	dB	$\sqrt{3}$	1	0.00018	100	$20log1 \pm 10^{\frac{R}{20}}$ $R = -70$
Mis	Mismatch	0.1	dB	$\sqrt{2}$	1	0.07071	100	$20log10(1 \pm \rho_1\rho_2)$
Cable	Cable screening and reflection	0	dB	$\sqrt{3}$	1	0	100	Negligible
RtoR	Range to range measurements, change in antenna	0.006	dB	$\sqrt{3}$	1	0.0035	100	Difference in measured values from one range to another range
Refl loss	Reflection from port to connection	0.5	dB	$\sqrt{2}$	1	0.356	100	
Mech	Measurement setup, level, same reference point	0	dB	$\sqrt{3}$	1	0	100	Negligible
Res	AUT resolution	0.05	dB	$\sqrt{3}$	1	0.0288	100	Max dB change in one frequency step
Data	ESDM of data	0.085	dB	1	1	0.085	100	ESDM of data
Uncertainty of measurement k = 2 95.45%						2.14	dB	

Table A6. Phase Uncertainty, frequency range 1 GHz – 5 GHz.

Symbol	Source of uncertainty	Estimated uncertainty	Unit	Probability distribution	Sensitivity coefficient	Standard uncertainty contribution	Reliability	Remarks
Std	Measured from anechoic chamber	5	deg	1	1	5	100	Max difference between FEKO and two antenna method were used
Range_ Refl	Compact range reflection	0	deg	$\sqrt{3}$	1	0	100	$20log1 \pm 10^{\frac{R}{20}}$ $R = -70$
Mis	Mismatch	0.6	deg	$\sqrt{2}$	1	0.4243	100	$\pm sin^{-1}\lvert\rho_1\rho_2\rvert$
Cable	Cable screening, reflection and phase variation	0	deg	$\sqrt{3}$	1	0	100	Negligible
RtoR	Range to range measurements, change in antenna	7	deg	$\sqrt{3}$	1	4.041	100	Difference in measured values from one range to another range
Refl loss	Reflection from port to connection	2	deg	$\sqrt{2}$	1	1.414	100	
Mech	Measurement setup, level, same reference point	5	deg	$\sqrt{3}$	1	2.887	100	Negligible
Phase	Fixed phase error	0	deg	$\sqrt{3}$	1	0		Was corrected for
Res	AUT resolution	2.75	deg	$\sqrt{3}$	1	1.588	100	Max degrees change in one frequency step
Data	ESDM of data	0.661	deg	1	1	0.661	100	ESDM of data
Uncertainty of measurement k = 2 95.45%						14.9	deg	

Table A7. Phase Uncertainty, frequency range 5 GHz – 7 GHz.

Symbol	Source of uncertainty	Estimated uncertainty	Unit	Probability distribution	Sensitivity coefficient	Standard uncertainty contribution	Reliability	Remarks
Std	Measured from anechoic chamber	5	deg	1	1	5	100	Max difference between FEKO and two antenna method were used
Range_ Refl	Compact range reflection	0	deg	$\sqrt{3}$	1	0	100	$20log1 \pm 10^{\frac{R}{20}}$ $R = -70$
Mis	Mismatch	0.6	deg	$\sqrt{2}$	1	0.4243	100	$\pm sin^{-1}\lvert\rho_1\rho_2\rvert$
Cable	Cable screening, reflection and phase variation	0	deg	$\sqrt{3}$	1	0	100	Negligible
RtoR	Range to range measurements, change in antenna	7	deg	$\sqrt{3}$	1	4.041	100	Difference in measured values from one range to another range
Refl loss	Reflection from port to connection	2	deg	$\sqrt{2}$	1	1.414	100	
Mech	Measurement setup, level, same reference point	10	deg	$\sqrt{3}$	1	5.774	100	Negligible
Phase	Fixed phase error	0	deg	$\sqrt{3}$	1	0		Was corrected for
Res	AUT resolution	2.75	deg	$\sqrt{3}$	1	1.588	100	Max degrees change in one frequency step
Data	ESDM of data	0.661	deg	1	1	0.661	100	ESDM of data
Uncertainty of measurement k = 2 95.45%						17.9	deg	

Table A8. Phase Uncertainty, frequency range 7 GHz – 8 GHz.

Symbol	Source of uncertainty	Estimated uncertainty	Unit	Probability distribution	Sensitivity coefficient	Standard uncertainty contribution	Reliability	Remarks
Std	Measured from anechoic chamber	5	deg	1	1	5	100	Max difference between FEKO and two antenna method were used
Range_ Refl	Compact range reflection	0	deg	$\sqrt{3}$	1	0	100	$20log1 \pm 10^{\frac{R}{20}}$ $R = -70$
Mis	Mismatch	0.6	deg	$\sqrt{2}$	1	0.4243	100	$\pm sin^{-1}\lvert\rho_1\rho_2\rvert$
Cable	Cable screening, reflection and phase variation	0	deg	$\sqrt{3}$	1	0	100	Negligible
RtoR	Range to range measurements, change in antenna	24	deg	$\sqrt{3}$	1	13.86	100	Difference in measured values from one range to another range
Refl loss	Reflection from port to connection	2	deg	$\sqrt{2}$	1	1.414	100	
Mech	Measurement setup, level, same reference point	10	deg	$\sqrt{3}$	1	5.774	100	Negligible
Phase	Fixed phase error	0	deg	$\sqrt{3}$	1	0		Was corrected for
Res	AUT resolution	2.75	deg	$\sqrt{3}$	1	1.588	100	Max degrees change in one frequency step
Data	ESDM of data	0.661	deg	1	1	0.661	100	ESDM of data
Uncertainty of measurement k = 2 95.45%						32	deg	

Table A9. Phase Uncertainty, frequency range 8 GHz – 10 GHz

Symbol	Source of uncertainty	Estimated uncertainty	Unit	Probability distribution	Sensitivity coefficient	Standard uncertainty contribution	Reliability	Remarks
Std	Measured from anechoic chamber	5	deg	1	1	5	100	Max difference between FEKO and two antenna method were used
Range_ Refl	Compact range reflection	0	deg	$\sqrt{3}$	1	0	100	$20log1 \pm 10^{\frac{R}{20}}$ $R = -70$
Mis	Mismatch	0.6	deg	$\sqrt{2}$	1	0.4243	100	$\pm sin^{-1}\lvert\rho_1\rho_2\rvert$
Cable	Cable screening, reflection and phase variation	0	deg	$\sqrt{3}$	1	0	100	Negligible
RtoR	Range to range measurements, change in antenna	0.8	deg	$\sqrt{3}$	1	0.462	100	Difference in measured values from one range to another range
Refl loss	Reflection from port to connection	2	deg	$\sqrt{2}$	1	1.414	100	
Mech	Measurement setup, level, same reference point	10	deg	$\sqrt{3}$	1	5.774	100	Negligible
Phase	Fixed phase error	0	deg	$\sqrt{3}$	1	0		Was corrected for
Res	AUT resolution	2.75	deg	$\sqrt{3}$	1	1.588	100	Max degrees change in one frequency step
Data	ESDM of data	0.661	deg	1	1	0.661	100	ESDM of data
Uncertainty of measurement k = 2 95.45%						16	deg	

Table A10. Phase Uncertainty, frequency range 10 GHz – 18 GHz.

Symbol	Source of uncertainty	Estimated uncertainty	Unit	Probability distribution	Sensitivity coefficient	Standard uncertainty contribution	Reliability	Remarks
Std	Measured from anechoic chamber	12	deg	1	1	12	100	Max difference between FEKO and two antenna method were used
Range_ Refl	Compact range reflection	0	deg	$\sqrt{3}$	1	0	100	$20log1 \pm 10^{\frac{R}{20}}$ $R = -70$
Mis	Mismatch	0.6	deg	$\sqrt{2}$	1	0.4243	100	$\pm sin^{-1}\lvert\rho_1\rho_2\rvert$
Cable	Cable screening, reflection and phase variation	0	deg	$\sqrt{3}$	1	0	100	Negligible
RtoR	Range to range measurements, change in antenna	0.2	deg	$\sqrt{3}$	1	0.115	100	Difference in measured values from one range to another range
Refl loss	Reflection from port to connection	2	deg	$\sqrt{2}$	1	1.414	100	
Mech	Measurement setup, level, same reference point	20	deg	$\sqrt{3}$	1	11.55	100	Negligible
Phase	Fixed phase error	0	deg	$\sqrt{3}$	1	0		Was corrected for
Res	AUT resolution	2.75	deg	$\sqrt{3}$	1	1.588	100	Max degrees change in one frequency step
Data	ESDM of data	0.661	deg	1	1	0.661	100	ESDM of data
Uncertainty of measurement k = 2 95.45%						33.7	deg	